Report No. 154.

LABORATORIUM VOOR SCHEEPSBOUWKUNDE

TECHNISCHE HOGESCHOOL DELFT

EQUATION OF MOTION COEFFICIENTS FOR A PITCHING AND HEAVING DESTROYER MODEL.

W.E. Smith .

September 1966.

Equation of Motion Coefficients for a Pitching and Heaving Destroyer Model.

W.E. Smith*

Abstract.

The equation of motion coefficients for a pitching and heaving destroyer model are measured using forced oscillation techniques. The forces due to waves on a constrained model are also measured. The pitch and heave motions in regular long crested head waves are measured. All coefficients, forces and motions are compared with results obtained from modified strip theory computation. Agreement in all cases is excellent.

* Physicist, David Taylor Model Basin, Washington, D.C. at Shipbuilding Laboratory, Delft on research assignment.

Introduction.

Formulation of the problem of calculating pitch and heave motions of a ship in head waves is now well established. The motions may be represented by a pair of coupled differential equations as developed by Korvin-Kroukovsky [1]. The validity of such a representation was established in a series of experiments by Gerritsma [2][3] [4] , in which each term of the equation was measured. The experiments employed a forced oscillation technique which permitted the measurement of the individual coefficients for a particular ship. The wave exciting forces on a constrained model were also measured. The experimentally derived coefficients and forces were then inserted into the equations and the motions computed. These computed motions were then compared with the results of a motion experiment in waves. Such results not only verified the validity of the differential equation representation, but in addition established the super position principle and the linearity of the motions. Subsequent to this, methods were developed which permitted the computer calculation of the coefficients and thus the motions. In the process of developing such a computer program, it was recognized that additional experimental information would be of considerable value in establishing the accuracy of such a calculation. Also, since the Gerritsma experiments were confined to one parent form of models, the 60 series, block .60, .70, and .80, with the major emphasis on the block .70, it was decided that experiments on an entirely different form would be desirable.

The computer computation of the motions employs a modified form of strip theory which has inherent assumptions that are in some ways similar to the assumptions for slender body theory. However, it should be observed that a ship moving with forward speed in the free surface is not approximated by either a two-dimensional slender body or an elongated slender body of revolution. In view of these somewhat tenuous similarities with slender body theory, and the possibility of future analytical relationships which may be based on slenderness assumption, a destroyer form was selected.

This form was much more slender than the relatively broad ship used in the Gerritsma [2] experiments. Also, since there were no large longitudinal slopes in the forward section of the ship, it was anticipated that experimental results from such a form when considered along with the 60 Series data, would provide information as to the importance of slenderness or longitudinal slope variations in strip theory computation.

Model Tested.

The model used for all tests was a conventional frigate hull of the Friesland class and was one for which the motion characteristics had been extensively investigated in full scale sea worthiness trials, (Bledsoe, Bussemaker and Cummins [5]). This model was constructed of fibreglass and was 2.81 m in length. For all testing the model was ballasted to the design load water line and was operated with a radius of gyration of .25 L_{oa} or .259 L_{pp}. This radius of gyration was selected to coincide with previous full scale trial conditions.

Table 1.

Main Particulars of Ship Model.

Scale ratio	40
Length L_{pp} M.	2.810
Beam M.	.2935
Draft (DWL) M.	.0975
Displacement KG	44.55
Block coeff.	.554
Midship area coeff.	.815
Prismatic coeff.	.679
Waterplane area coeff.	.798
L. centre of mass M $\frac{L_{pp}}{2}$	.0293 AFT
Radius of gyration pitch	.259 L_{pp}

1. Force Oscillation Test - Heave.

The model was force oscillated in heave using the Delft Shipbuilding Laboratory mechanical oscillator [10]. The model was attached to the oscillator by means of two force transducers, as shown in Figure 1. The oscillator employed a Scotch-yoke mechanism to impart a constant frequency, sinusoidal motion to the model. The frequency capabilities of the oscillator were such that oscillation tests could be performed at any discreet frequency between $\omega = 2$ and $\omega = 15$. It was also possible to vary the oscillation amplitude and for this test amplitudes of .01 m, .02 m, and .04 m were used. Heave test conditions are summarized in Table 2.

Table 2.

Heave Oscillation Test Conditions.

Speed	F_n = .15, .25, .35, .45, .55
Frequency range	$\omega_e\sqrt{\frac{L_{pp}}{g}} = 1$ to $\omega_e\sqrt{\frac{L_{pp}}{g}} = 8$
Amplitude	Z_a = .01, .02, .04 m.

For this experiment the model was oscillated vertically and the vertical force required to sustain steady state oscillation was measured with a transducer in the bow and stern of the model. See Fig. 1. The sum of the forces of the forward and aft transducers is the total heave force, and the difference represents the heave into pitch coupling terms which is due to asymmetries in the hydrostatic and hydrodynamic forces on the model. The force transducer outputs were connected directly to an analog Fourier analyzer which provided a direct indication of the in phase and out of phase component of the first or fundamental harmonic of the forces. The higher harmonic content of the signal, if any, was not measured.

2. Force Oscillation Experiment Pitch.

The ship model was force oscillated in pitch only at a number of frequencies and amplitudes, as shown in Table 3.

Table 3.

Pitch Oscillation Test Conditions.

Speed	F_n = .15, .25, .35, .45, .55
Frequency range	$\omega_e\sqrt{\frac{L_{pp}}{g}} = 1$ to $\omega_e\sqrt{\frac{L_{pp}}{g}} = 8$
Amplitude	θ_a = .01, .02, .04 radians.

The measuring apparatus was identical with that for heave.

3. Wave Excitation Force Experiment.

The ship model was rigidly attached to the carriage by two fore and aft mounted force transducers which permitted the measurement of the forces exerted on the stationary model by the incident waves.

The waves were regular long-crested and were approximately $L_{pp}/40$ in height. Wave lengths were varied from $L_{pp}/\lambda = .5$ to $L_{pp}/\lambda = 2.0$. The forces and moments on the model due to the waves were recorded on an ultra-violet strip chart recorder. Simultaneously, the wave height was measured using a resistance wire probe, mounted four meters forward of the model's centre of gravity and directly ahead of the model. This data was also recorded on the ultra-violet strip chart recorder.

The information recorded was analyzed manually by averaging the value for ten consecutive cycles of motion. For the wave height measurement, the phases relative to the forces were adjusted to compensate for the distance between the wave probe location and the model centre of gravity. Test conditions are as shown in Table 4.

Table 4.

Wave Excitation Force Test Conditions.

Speed	F_n = .15, .25, .35, .45, .55
Wave length ratio	L_{pp}/λ = .500, .555, .625, .714, .833, 1.000, 1.250, 1.670, 2.000
Wave height ratio	$2\zeta_a/L_{pp} = \frac{1}{40}$

4. Motion Experiments.

The unpowered model was connected to a towing apparatus which was so arranged as to restrict all modes of motion except pitch and heave. All testing was done in regular long crested head waves with a peak height of approximately $L_{pp}/40$. The wave heights were reduced at frequencies nears resonance to prevent the model from shipping water. The wave lengths were varied from L_{pp}/λ = .5 to L_{pp}/λ = 2.0.

Pitch, heave and wave displacements were recorded for each test condition. The pitch and heave displacements were sensed by micro-torque rotary potentiometers mounted as part of the towing apparatus. The towing strut and motion transducers were arranged so that the restraint forces in heave and pitch were negligible. The wave height was sensed by a resistance wire probe located four meters forward of the model's centre of gravity and directly ahead of the model. All data was recorded simultaneously on a multi channel ultra-violet strip chart recorder. Motion information was recorded only after the carriage and model had been running at a constant speed for a sufficient length of time to insure steady state conditions.

The information recorded was analyzed manually by averaging the values of ten consecutive cycles of motion. For the wave height measurement, the phases relative to the motions were adjusted to compensate for the distance between the wave probe location and the model centre of gravity.

Model test conditions are shown in Table 5.

Table 5.

Motion Test Conditions.

Speed	$Fn = .15,\ .25,\ .35,\ .45,\ .55.$
Wave length ratio	$L_{pp}/\lambda = .500,\ .555,\ .625,\ .714,\ .833,\ 1.000,\ 1.250,\ 1.670,\ 2.000$
Wave height ratio	$2\zeta_a/L_{pp} = 1/40$

Each of the above tests were performed at the speeds Fn .15, .25, .35, .45 and .55.

5. Analysis Forced Oscillation.

Selecting a standard right handed coordinate system as shown in Fig. 21, the equations of motion for pitch and heave in head waves are:

$$(a+\rho\nabla)\ddot{z}+b\dot{z}+cz-d\ddot{\theta}-e\dot{\theta}-g\theta = F_a\cos(\omega_e t+\varepsilon_{F\zeta})$$

$$(A+\rho\nabla k^2_{yy})\ddot{\theta}+B\dot{\theta}+C\theta-D\ddot{z}-E\dot{z}-Gz = M_a\cos(\omega_e t+\varepsilon_{M\zeta})$$

Inherent in such a representation are the usual assumptions of superposition and that coupling from other modes of motion is small. For head waves such a coupling assumption is apparently justified.

To experimentally evaluate the coefficients it is necessary to perform two linearily independent experiments at each frequency and measure the exciting force, moment and displacements.

For simplicity of computation the two experiments can be designed so that only one mode of motion is present in each experiment.

The resulting equations for the heave experiments are:

$$(a+\rho\nabla)\ddot{z}+b\dot{z}+cz = F_z\cos(\omega_e t+\varepsilon_{F1})$$

$$D\ddot{z}+E\dot{z}+Gz = -M_z\cos(\omega_e t+\varepsilon_{M1})$$

For a forced heaving motion:

$$z = z_a\cos\omega_e t\ ,$$

the coefficients may be expressed as:

$$a = \frac{C Z_a - F_Z \cos\varepsilon_{FZ}}{Z_a \omega_e} - \rho\nabla$$

$$b = \frac{F_Z \sin\varepsilon_{FZ}}{Z_a \omega_e}$$

$$D = \frac{G Z_a + M_Z \cos\varepsilon_{MZ}}{Z_a \omega_e^{2}}$$

$$E = \frac{-M_Z \sin\varepsilon_{MZ}}{Z_a \omega_e}$$

The pitch experiment equations are:

$$d\ddot{\theta} + e\dot{\theta} + g\theta = -F_\theta \cos(\omega_e t + \varepsilon_{F\theta})$$

$$\bar{A}\ddot{\theta} + B\dot{\theta} + C\theta = M_\theta \cos(\omega_e t + \varepsilon_{M\theta})$$

For a forced pitching motion:

$$\theta = \theta_a \cos \omega_e t$$

the remaining coefficients are:

$$\bar{A} = \frac{C\theta_a - M_\theta \cos\varepsilon_{M\theta}}{\theta_a \omega_e^{2}}$$

$$B = \frac{M_\theta \sin\varepsilon_{M\theta}}{\theta_a \omega_e}$$

$$\bar{d} = \frac{g\theta_a + F_\theta \cos\varepsilon_{F\theta}}{\theta_a \omega_e^{2}}$$

$$e = \frac{-F_\theta \sin\varepsilon_{F\theta}}{\theta_a \omega_e}$$

6. Analysis wave forces.

The force and moment on the totally restrained model;

$$F_W = F_a \cos(\omega_e t + \varepsilon_{F\zeta})$$

$$M_W = M_a \cos(\omega_e t + \varepsilon_{M\zeta})$$

This measurement then provided the relationship between the wave shape and the force and moment exerted on the model.

Discussion.

The oscillator experiment provided measured values for all eight of the dynamic coefficients (a, b, $\bar{d}$, e, $\bar{A}$, B, D, E) of the equation of motion. The coefficients were measured for several amplitudes of the motion; for heave, 10, 20 and 40 percent of the designed draft, and for pitch, the vertical motion of the bow was 14, 28 and 56 percent of the designed draft. The coefficient values obtained for the different amplitudes showed only minor differences and would, to a certain extent, indicate good linearity.

It must be remembered, however, that a Fourier analysis was performed on all test information and only the first harmonic component was retained. Under such circumstances, the Fourier analyzer can in itself act as a linearizing device which could mask certain types of non linearity. Therefore, it cannot be said that such an experiment is a complete verification of linearity. Such a final verification of linearity must of necessity await the completion of the analysis of a transient or similar oscillator experiment in which higher harmonics are considered. The experimental results for the different amplitudes are shown in the Figures 1 through 10.

The coefficients were also calculated using a computer program which employs a modified form of strip theory. This program uses the Ursell [6] solution for a circular cylinder and the conformal transformation of the circular cylinder into shiplike form, Tasai [7] Porter [8] . For the computer computations two methods were tried: (1) using a Lewis form or three coefficient transformation of the cylinder and, (2) a so-called close fit program involving an arbitrary number of transformation coefficients.

The Lewis form for three coefficient transformations is one which approximates the shape of the ship sections with an elliptic curve which matches the beam, the draft and the area of the shiplike section exactly. While this is in general not a good approximation for ship sections, it fits the particular destroyer considered here very well. Therefore, any differences between a Lewis form and close fit computation should be small.

The Lewis form computed values for the coefficients are shown in the figures along with the experimental results. In every case experimental results and computation agree quite well, with the best agreement for the main added mass and damping term. The cross coupling terms generally show good agreement with the speed dependency clearly evident in the damping terms (e, E). The speed dependency normally associated with the restoring force terms (g, C), which for ease of analysis has been arbitrarily included in the added mass term ($\bar{d}$, $\bar{A}$), is also clearly evident in both computation and experiment. The absence of speed dependency for the terms (a, b, B, D) is also clearly demonstrated. The agreement over all appears to be considerably better than that for the Series 60 block 70 data as reported by Gerritsma [9].

This is consistent with slender body assumptions and indicates that such assumptions may indeed be applicable to surface ship computations using modified strip theory. Assuming that such a relationship exists, the satisfactory agreement between computation and experiment for both the Series 60 block 70 and the Friesland destroyer is an indication of the large deviation from a true slender body which are possible while still maintaining satisfactory computational accuracy.

The close fit or multi transformation coefficient program was also used to compute the equation of motion coefficient terms. The differences if any, from the Lewis form computations were small. This is not surprising since for this ship the Lewis form transformation is a good fit. While the differences from a ship design standpoint are insignificant, it is interesting to note that in every case where a difference occurred the close fit data showed improved agreement with experiments. The close fit computation values, where different from the Lewis form computations, are also shown in the figures with the experimental coefficients.

The wave exciting forces and moments were also measured. These are shown in Figures 11 through 15. Agreement between the measured exciting forces and moments and computation is excellent, with only small deviation at the higher frequency. A comparison of the phase angles shows good agreement between computation and experiment at low and medium frequencies only, i.e. below $L_{pp}/\lambda = 1.0$.

Agreement between experiment and computation for the motions, amplitudes and phase angles is excellent. The only difference of any significance occurs in the heaving motion at the higher wave frequencies, that is near $L_{pp}/\lambda = 1.5$. The motions, however, at this frequency are so small that this difference is not considered to be important.

Conclusions.

The ability of modified strip theory to account for forward speed effects even to the relatively high Froude number of .55 is demonstrated.

When the results from this experiment and the Gerritsma Series 60 experiments are compared an estimate of the importance of deviations from the slender body assumptions is possible.

The capabilities of a computer program based on modified strip theory for the computation of pitch and heave motions in head waves is demonstrated.

The agreement between computed and experimental motions provides still another demonstration of the linearity of this problem.

Acknowledgement.

This work was made possible through the cooperation and support of the Studiecentrum T.N.O. voor Scheepsbouw en Navigatie.

Particular appreciation is expressed for an objective evaluation of the research aims of this project to Mr. W. Spuyman

The excellent computation assistance provided by the Wiskundige Dienst (Computer Department) is greatfully acknowledged.

Timely completion of this project was made possible by the enthusiatic assistance of the Shipbuilding Laboratory Staff.

Nomenclature.

a b c d e g A B C D E G	- Coefficients of the equations of motion for heave and pitch.
C_B	- Block coefficient.
F_z	- Force on model due to forced heave motion.
F_θ	- Force and model due to forced pitch motion.
F_a	- Wave force amplitude on restrained model.
$Fn = \frac{V}{\sqrt{gL_{pp}}}$	- Froude number.
g	- Acceleration due to gravity.
k_{yy}	- Radius of gyration of model in pitch.
L_{oa}	- Length over all.
L_{pp}	- Length between perpendiculars.
M_a	- Total moment amplitude on model.
M_w	- Wave moment amplitude on restrained ship.
M_z	- Moment on model due to forced heave motion
M_θ	- Moment on model due to forced pitch motion.
t	- Time.
x_b, y_b, z_b	- Right-handed body axis system.
z	- Heave displacement.
z_a	- Heave amplitude
ε	- Phase angle between the motions (forces, moments) and the waves.
ζ	- Instantaneous wave elevation.
ζ_a	- Wave amplitude.
θ_a	- Pitch amplitude.
λ	- Wave length.
ρ	- Density of water.
∇	- Displacement of volume.
ω	- Circular frequency.
ω_e	- Circular frequency of encounter.
θ	- Pitch angle.

References.

1 B.V. Korvin-Kroukovsky, W.R. Jacobs.
"Pitching and Heaving Motions of a Ship in Regular Waves", Transactions Society of Naval Architects and Marine Engineers, 1957.

2 J. Gerritsma.
"Ship Motions in Longitudinal Waves", International Shipbuilding Progress, 1960.

3 J. Gerritsma W. Beukelman.
"Distribution of the Hydrodynamic Forces on a Heaving and Pitching Ship Model in Still Water", International Shipbuilding Progress, 1964.

4 J. Gerritsma, W.E. Smith,
"Full Scale Destroyer Motion Measurements", Laboratorium voor Scheepsbouwkunde, Technische Hogeschool-Delft, Report No. 142, 1966.

5 M.D. Bledsoe, O. Bussemaker, W.E. Cummins.
"Seakeeping Trials on Three Dutch Destroyers", Transactions Society of Naval Architects and Marine Engineers, 1960.

6 F. Ursell.
"On the Heaving Motion of a Circular Cylinder on the Surface of a Fluid", Quarterly Journal Mech. and Applied Math. Vol. II PT2 1949.

7 F. Tasai,
"On the Damping Force and Added Mass of Ships Heaving and Pitching", Report of Research Institute for Applied Mechanics,Kyushu University, 1960.

8. W.R. Porter,
"Pressure Distribution, Added Mass and Damping Coefficients for Cylinders Oscillating in a Free Surface", University of California, Institute of Engineering Research, Series 82, 1960.

9 J. Gerritsma,
"Distribution of Hydrodynamic Forces along the Length of a Ship Model in Waves", Laboratorium voor Scheepsbouwkunde, Technische Hogeschool-Delft, Report No. 144, 1966.

10 H.J. Zunderdorp, M. Buitenhek,
Oscillator-Techniques at the Shipbuilding Laboratory", Laboratorium voor Scheepsbouwkunde, Technische Hogeschool-Delft, Report No. 111, 1963.

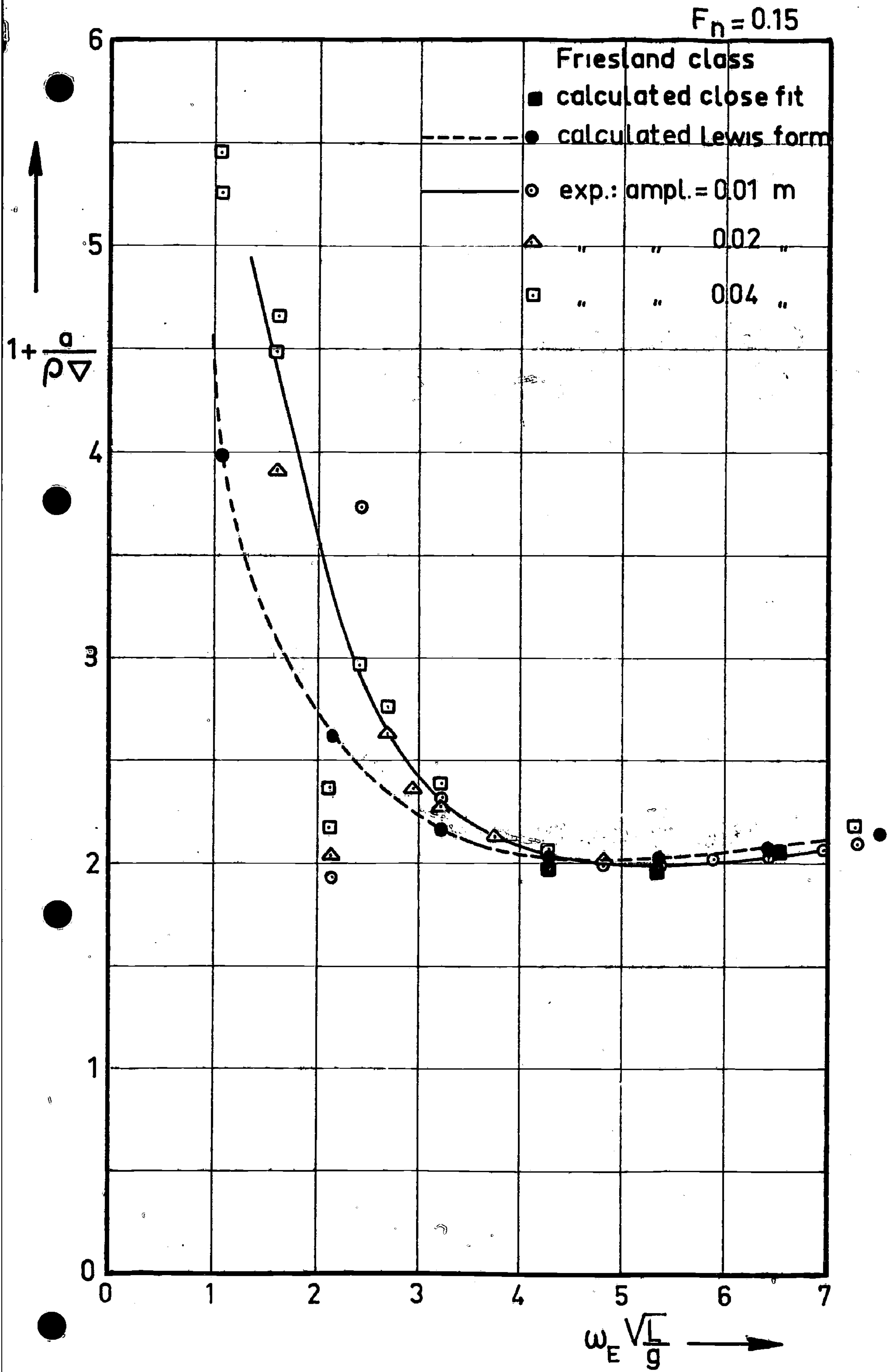

$F_n = 0.15$
Friesland class
calculated close fit
calculated Lewis form
exp.: ampl. = 0.01 m
" " 0.02 "
" " 0.04 "
$1+\frac{a}{\rho\nabla}$
$\omega_E\sqrt{\frac{L}{g}}$
0
1
2
3
4
5
6
7

FIG: 1 A

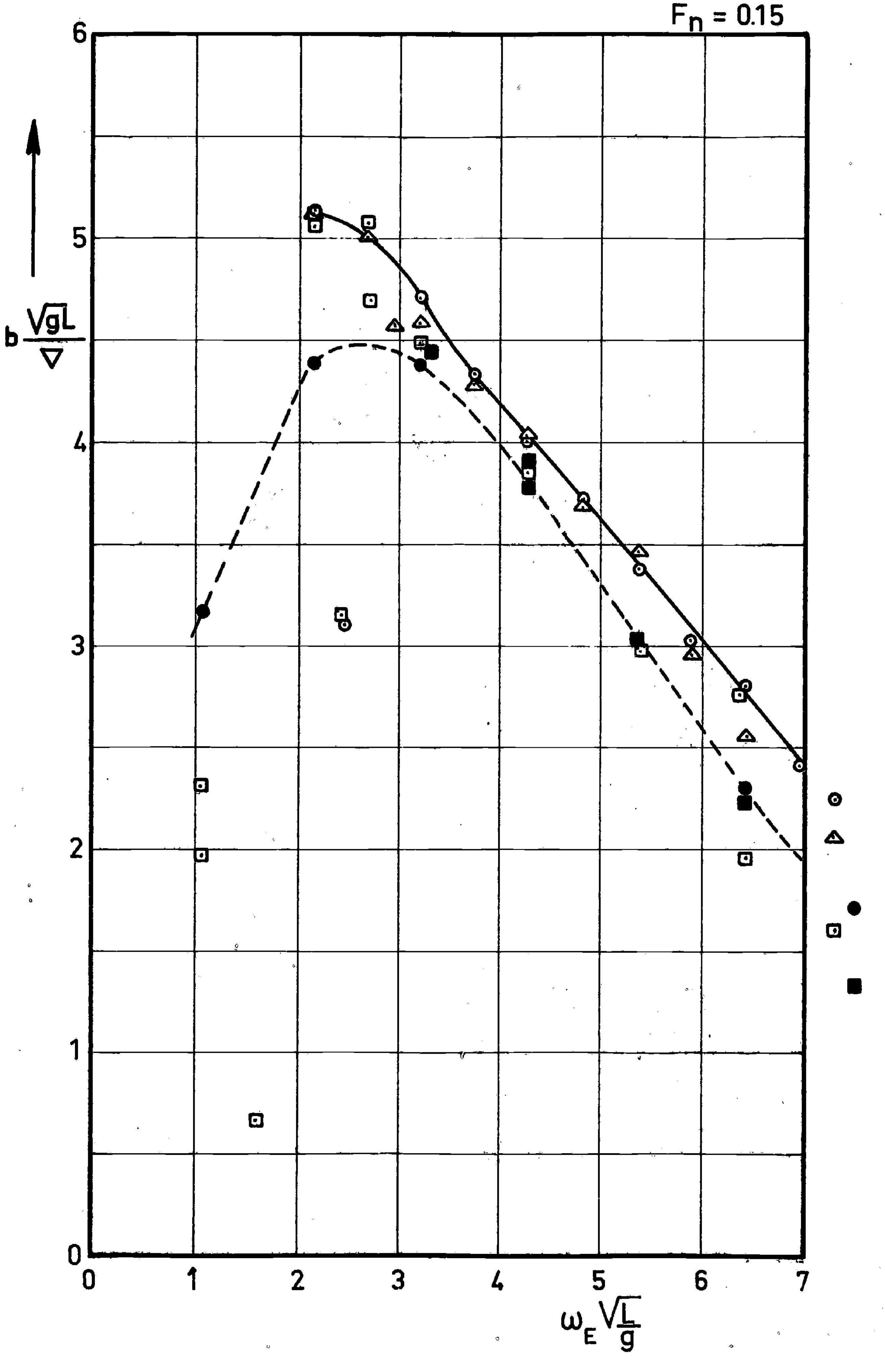

FIG: 1 B

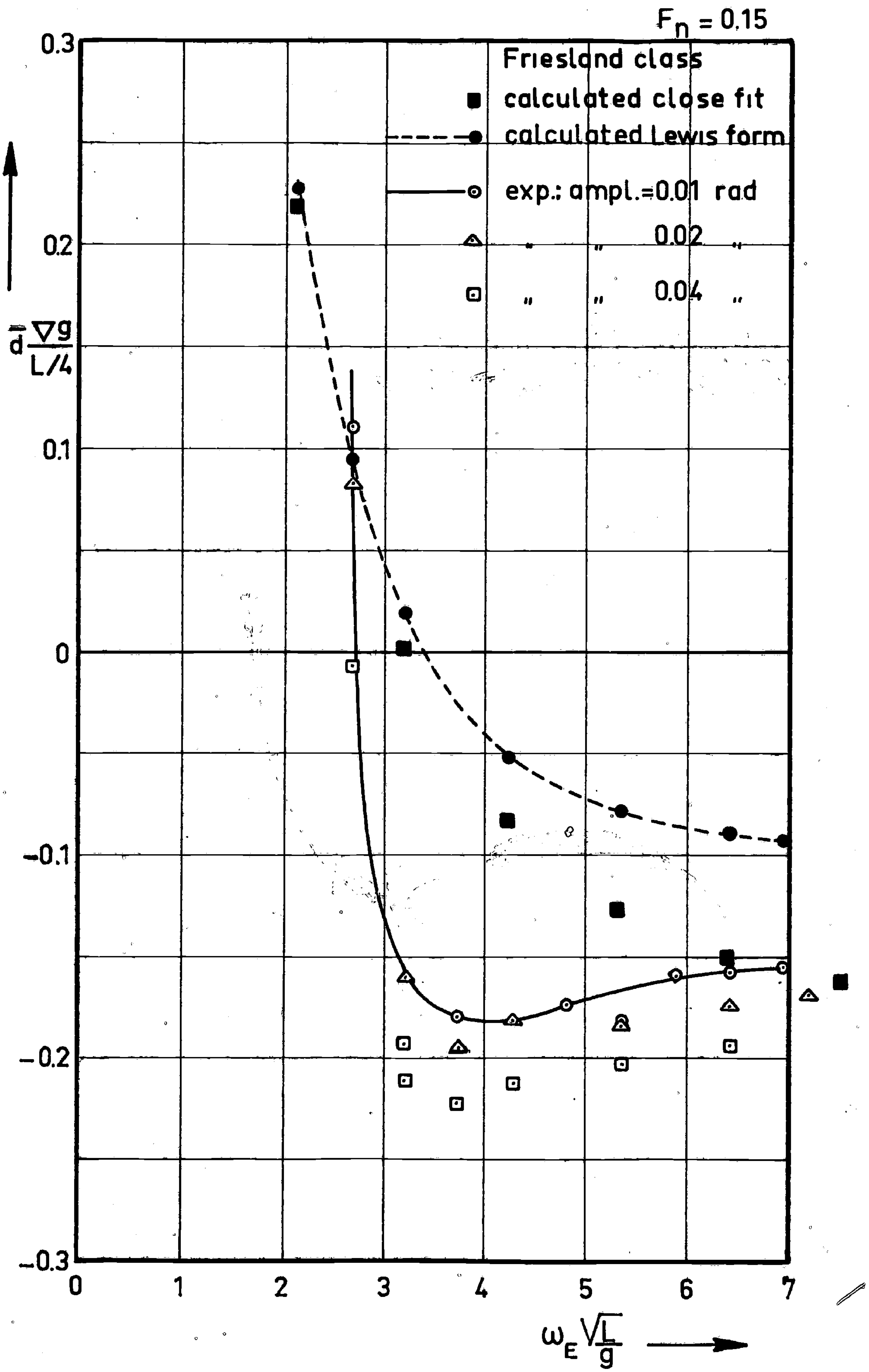

$F_n = 0.15$
Friesland class
calculated close fit
calculated Lewis form
exp.: ampl.=0.01 rad
" " 0.02 "
" " 0.04 "
0.3
0.2
0.1
0
−0.1
−0.2
−0.3
$\bar{d}\frac{\nabla g}{L/4}$
0
1
2
3
4
5
6
7
$\omega_E\sqrt{\frac{L}{g}}$

FIG: 1C

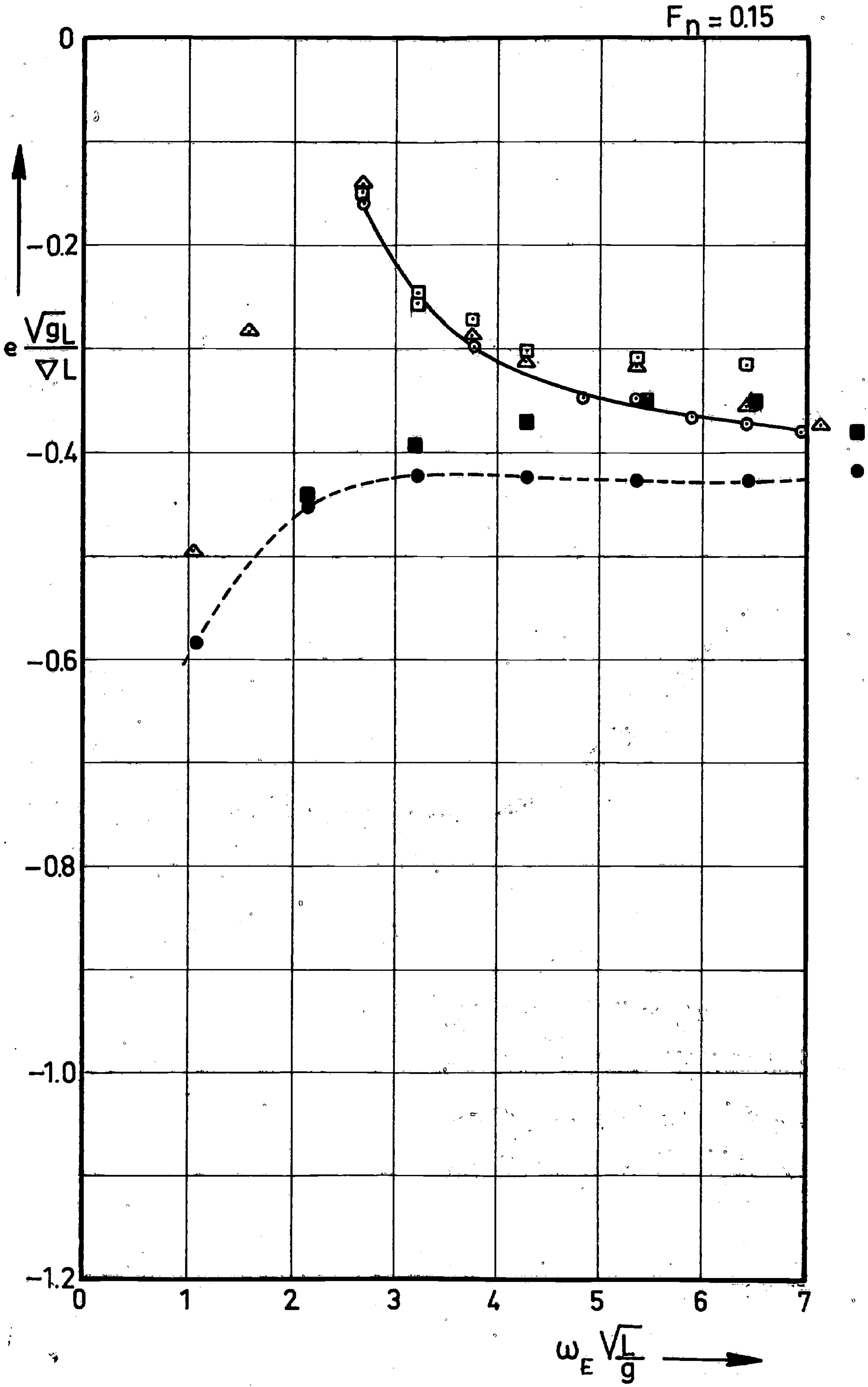

$F_n = 0.15$
0
−0.2
−0.4
−0.6
−0.8
−1.0
−1.2
$e\frac{\sqrt{gL}}{\nabla L}$
0
1
2
3
4
5
6
7
$\omega_E\sqrt{\frac{L}{g}}$

FIG: 1D

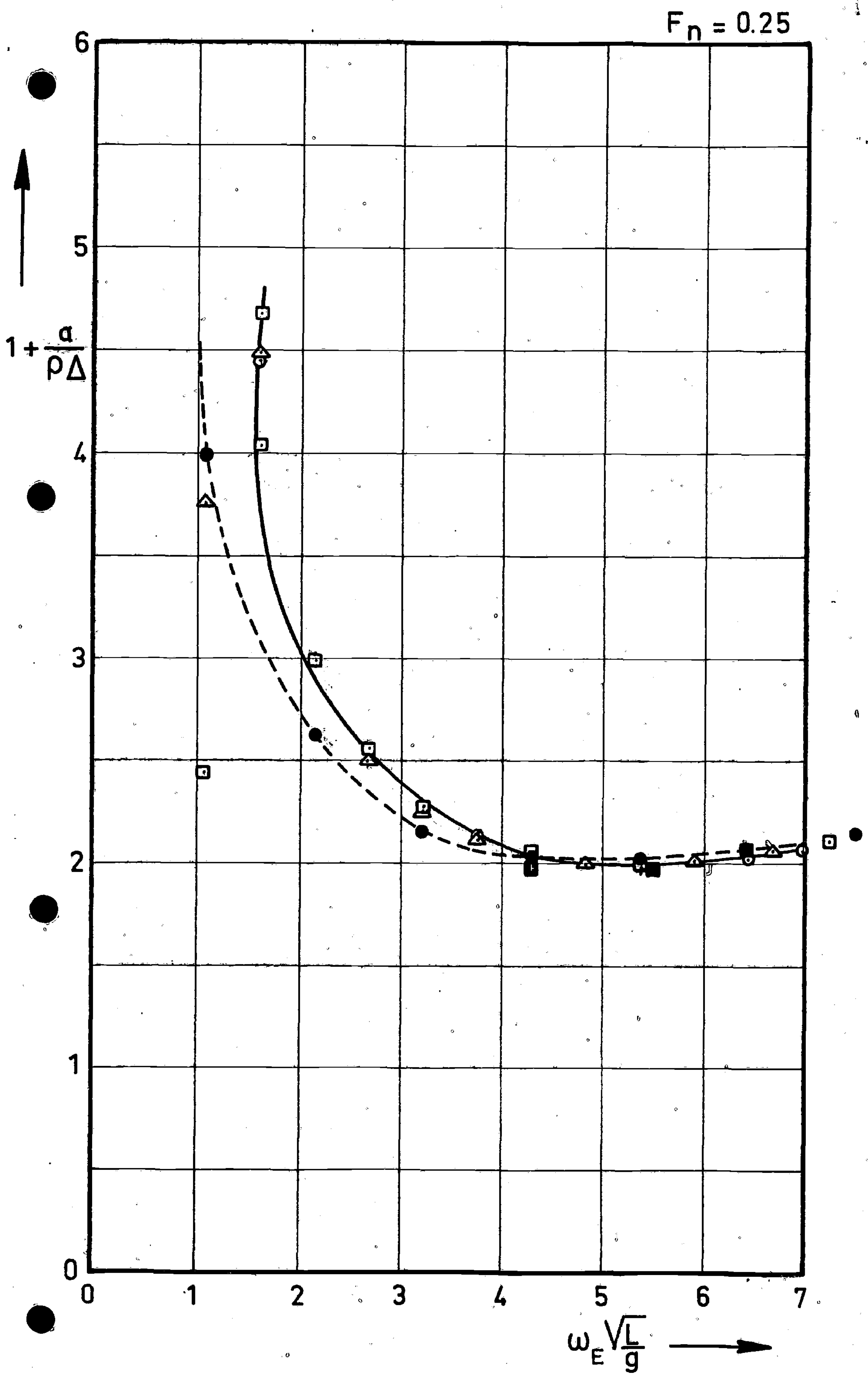

FIG : 2 A.

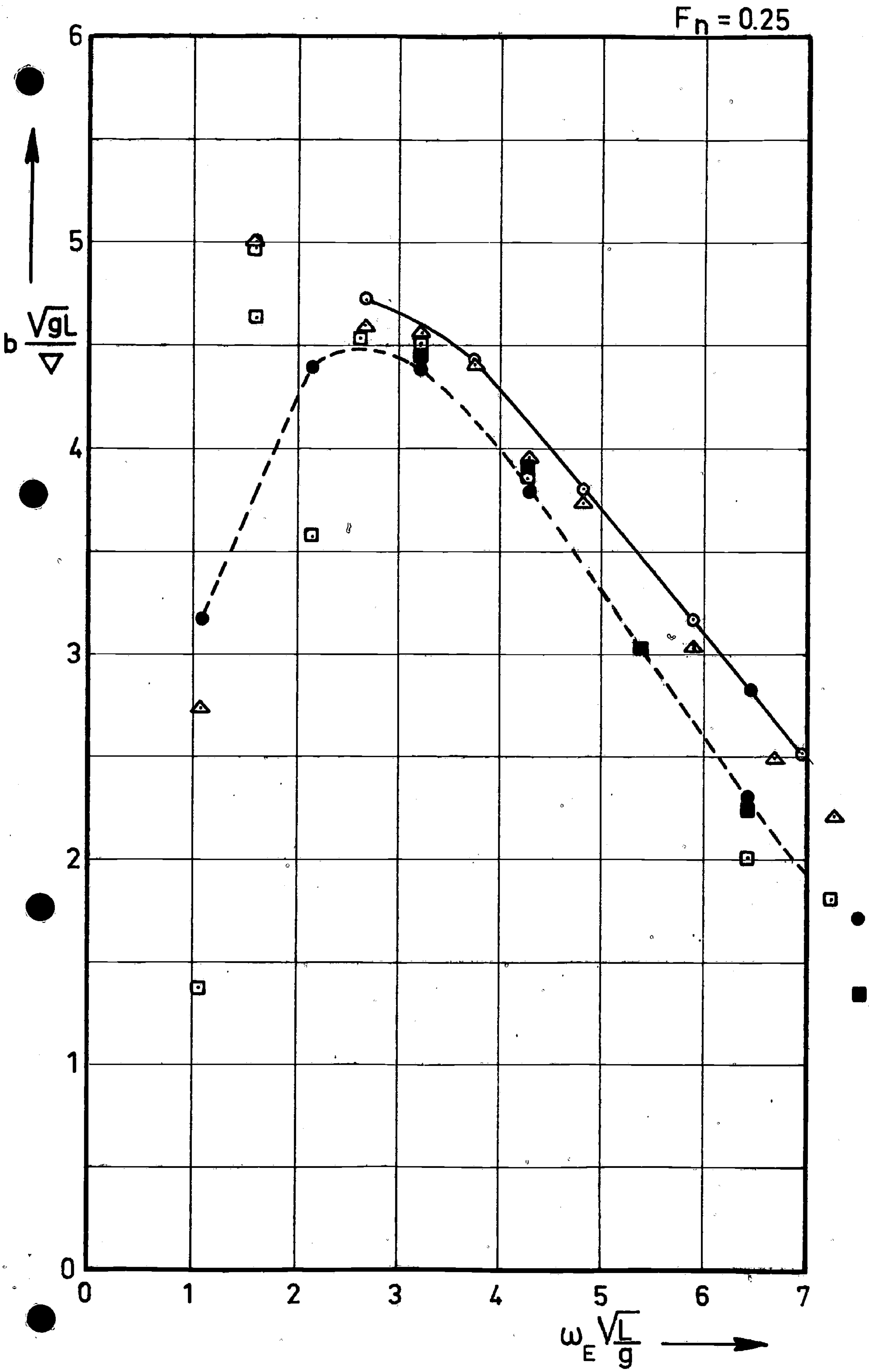

FIG: 2 B

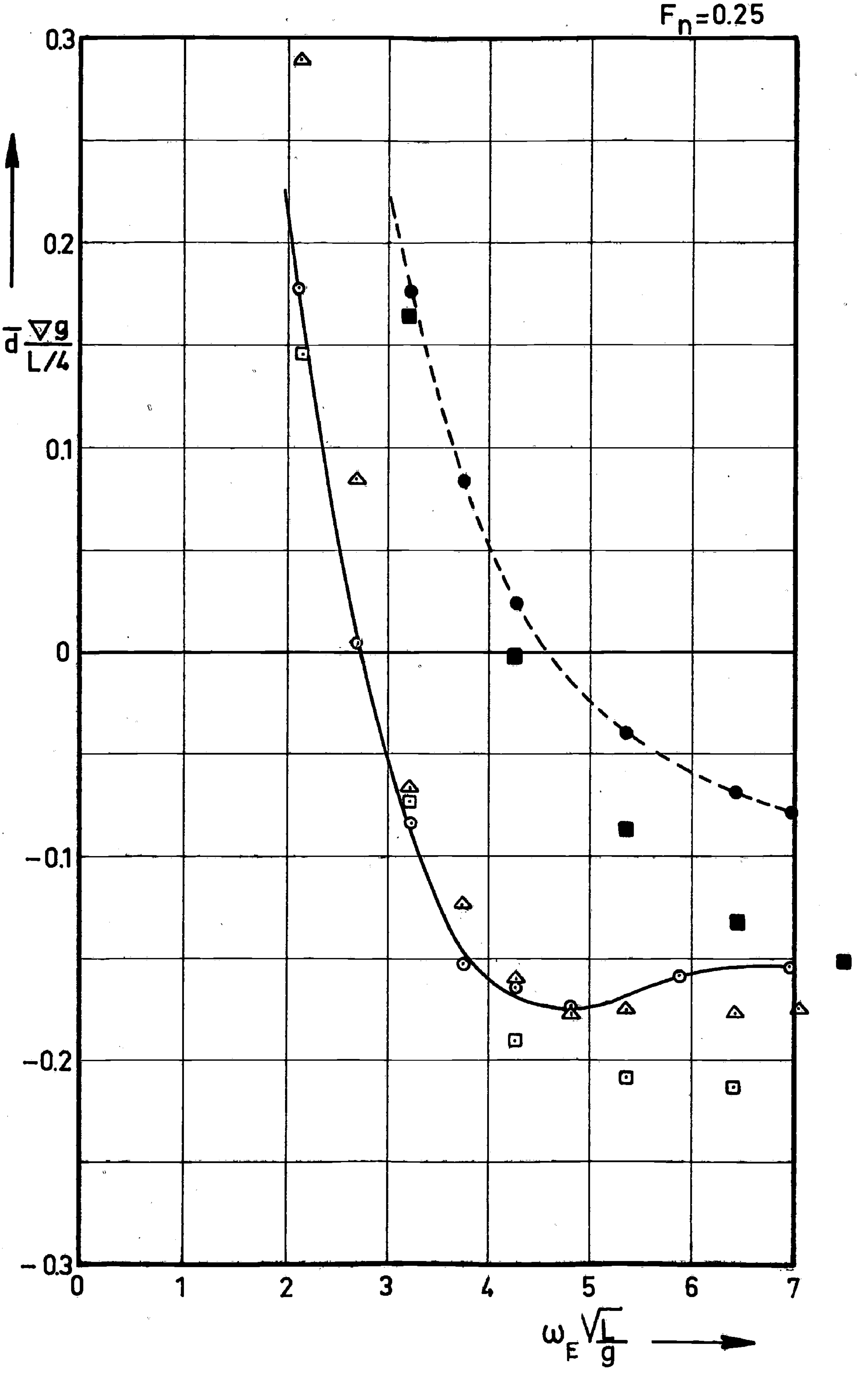
F_n=0.25
0.3
0.2
0.1
0
-0.1
-0.2
-0.3
$\bar{d}\,\frac{\nabla g}{L/4}$
0
1
2
3
4
5
6
7
$\omega_E\sqrt{\frac{L}{g}}$

FIG 12 C

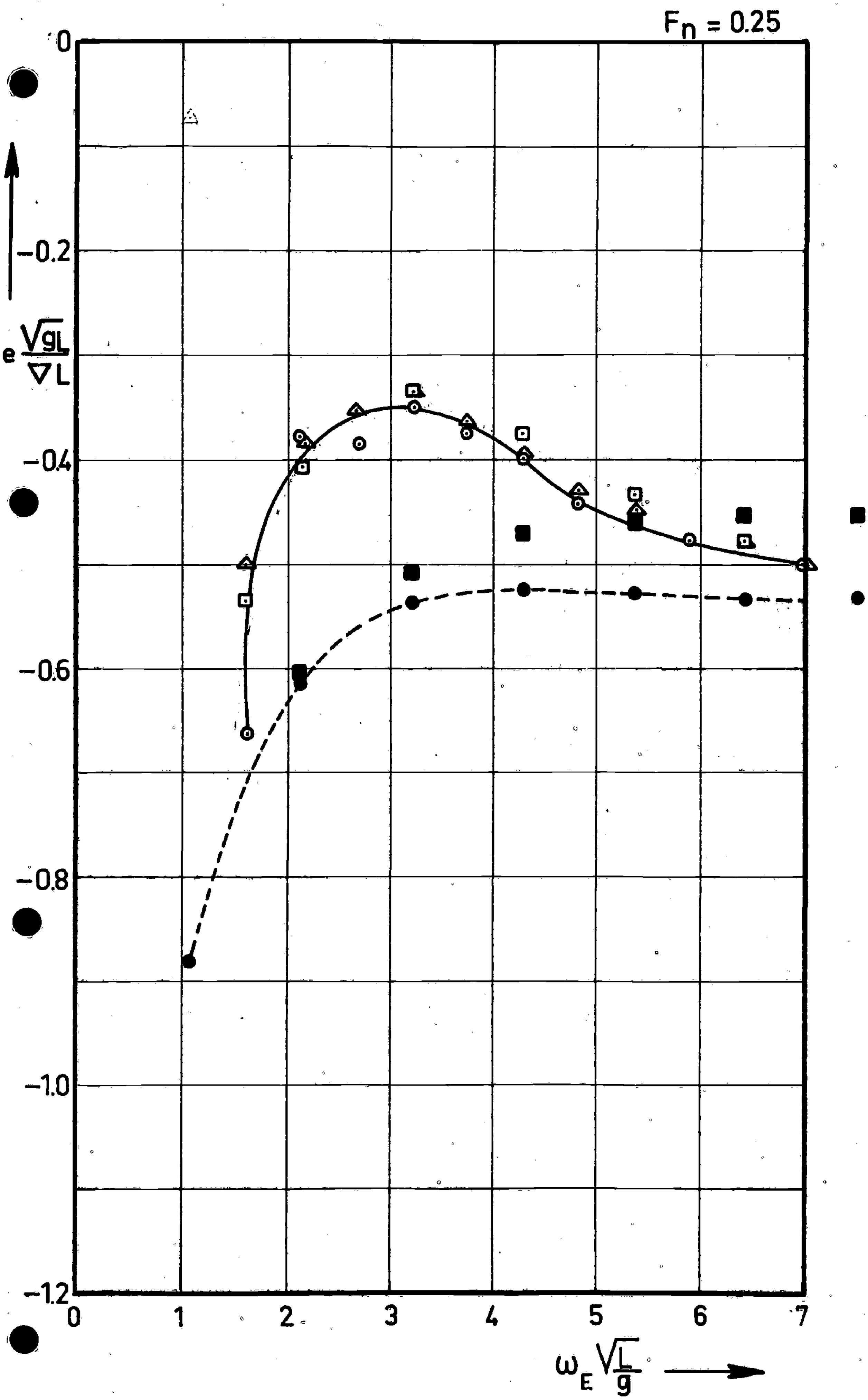

FIG: 2 D

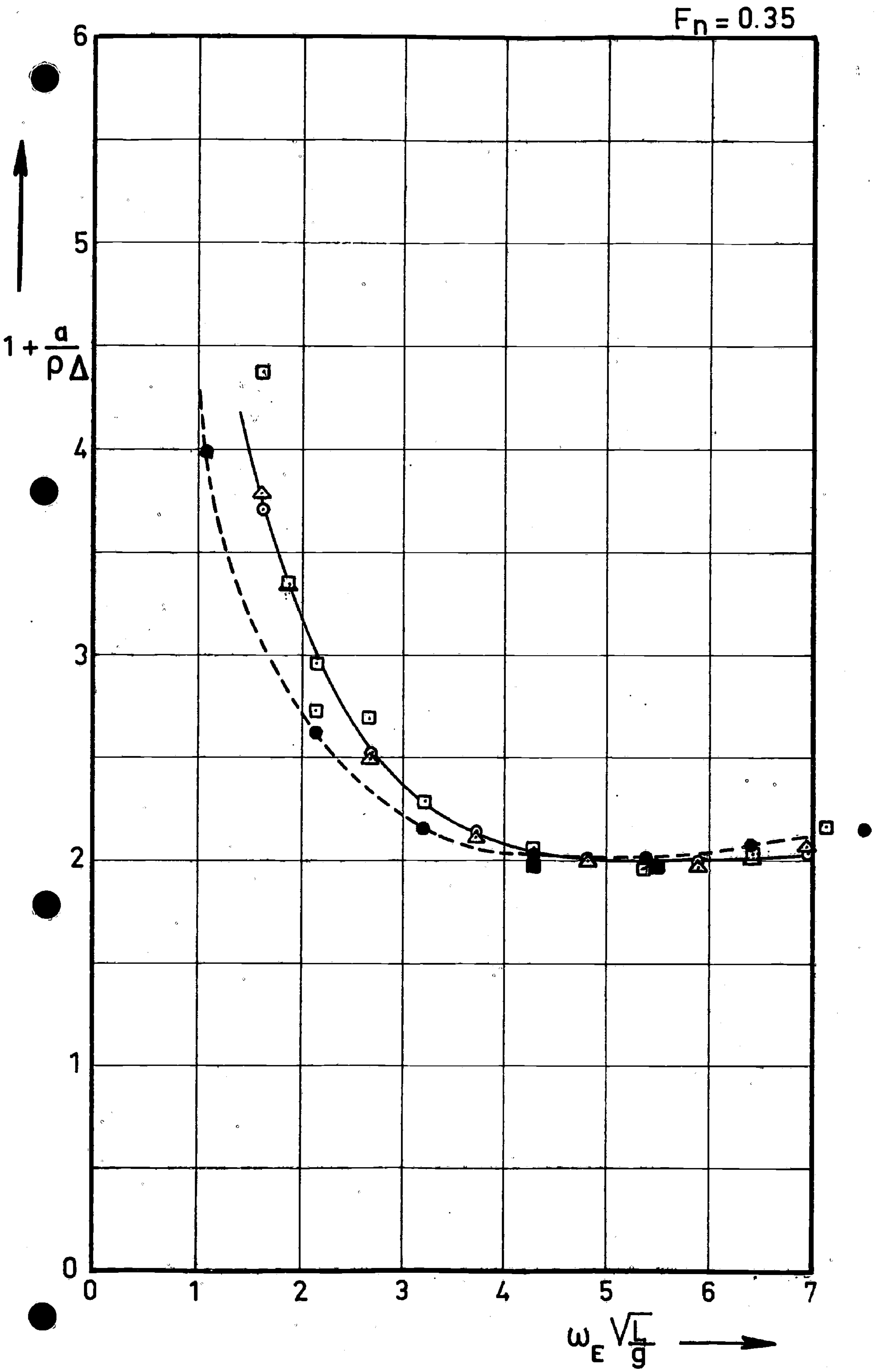

$F_n = 0.35$
$1 + \frac{a}{\rho \Delta}$
6
5
4
3
2
1
0
0
1
2
3
4
5
6
7
$\omega_E \sqrt{\frac{L}{g}}$

FIG: 3 A.

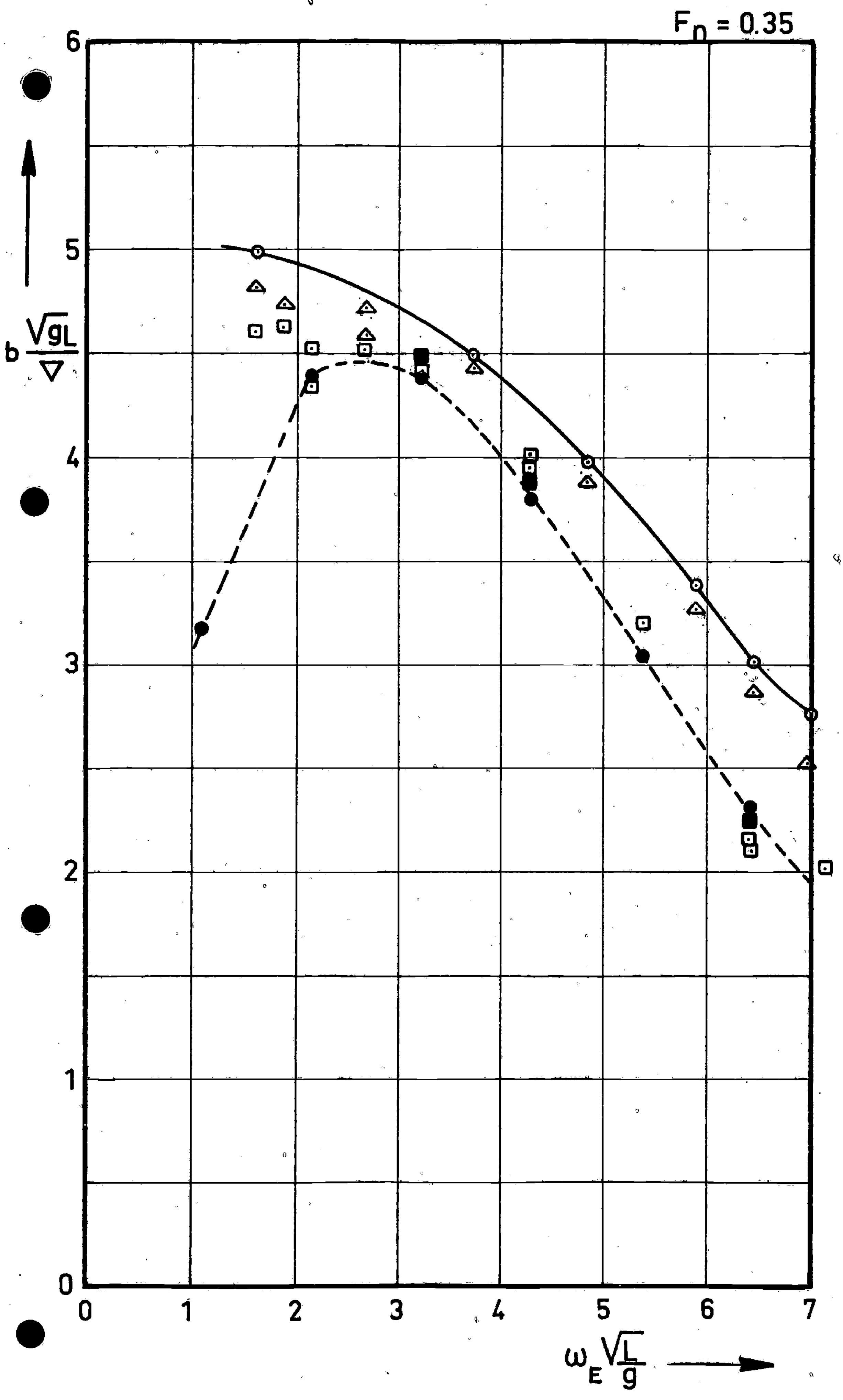

FIG: 3B

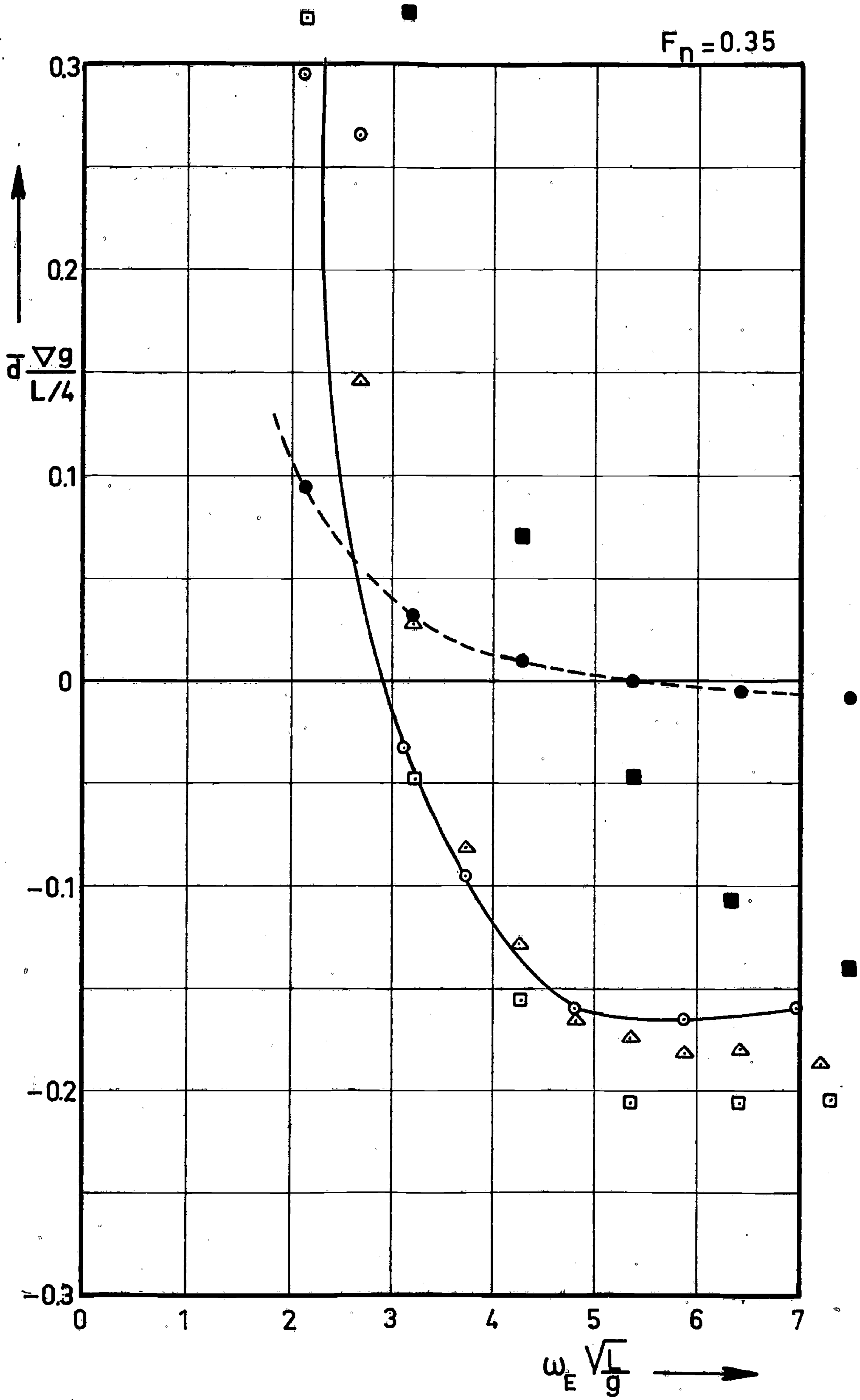

$F_n = 0.35$
0.3
0.2
0.1
0
-0.1
-0.2
-0.3
$\bar{d}\frac{\nabla g}{L/4}$
0
1
2
3
4
5
6
7
$\omega_E\sqrt{\frac{L}{g}}$

FIG: 3C

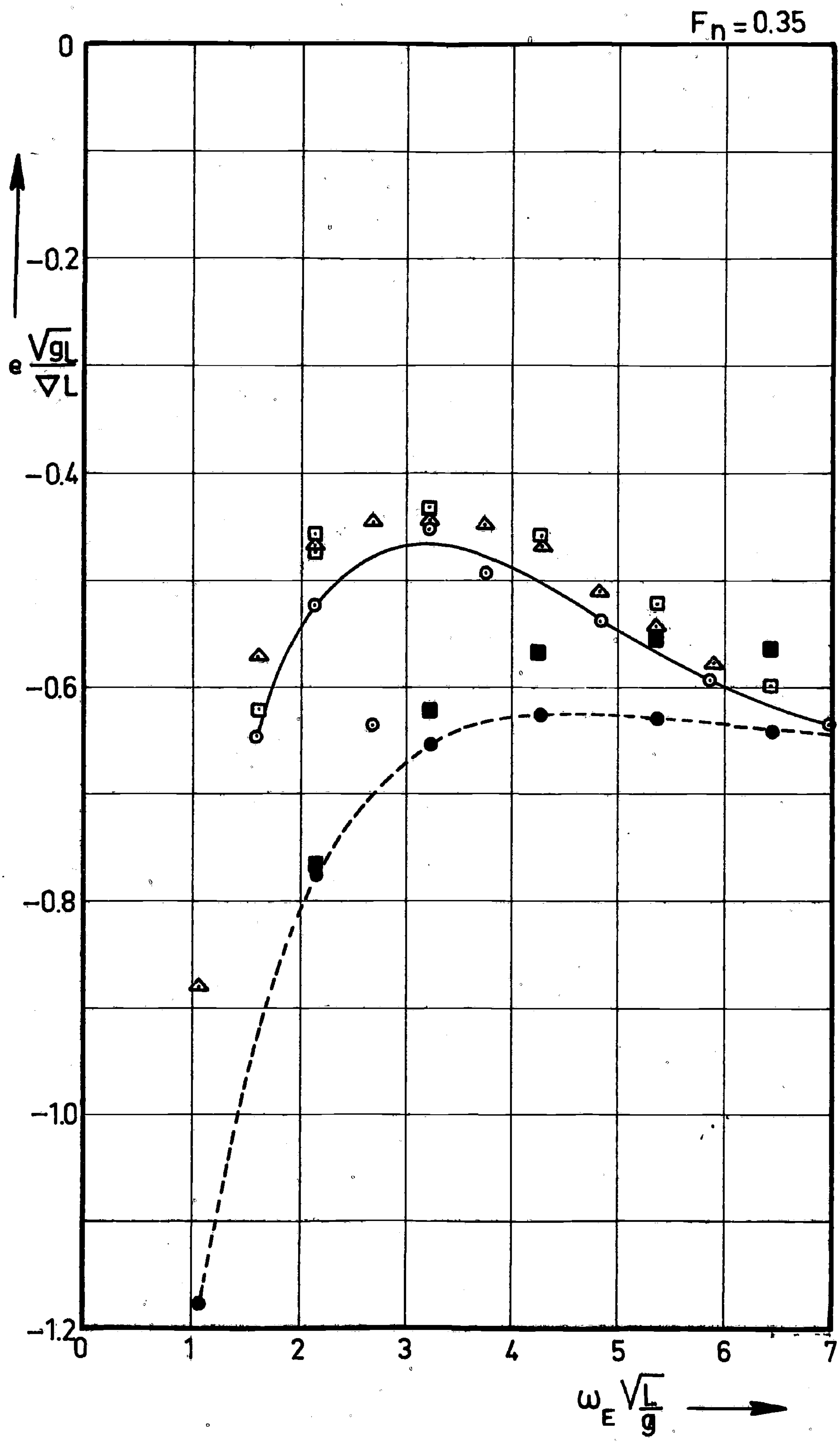
$F_n = 0.35$
0
−0.2
−0.4
−0.6
−0.8
−1.0
−1.2
$e\frac{\sqrt{gL}}{\nabla L}$
0
1
2
3
4
5
6
7
$\omega_E\sqrt{\frac{L}{g}}$

FIG: 3 D

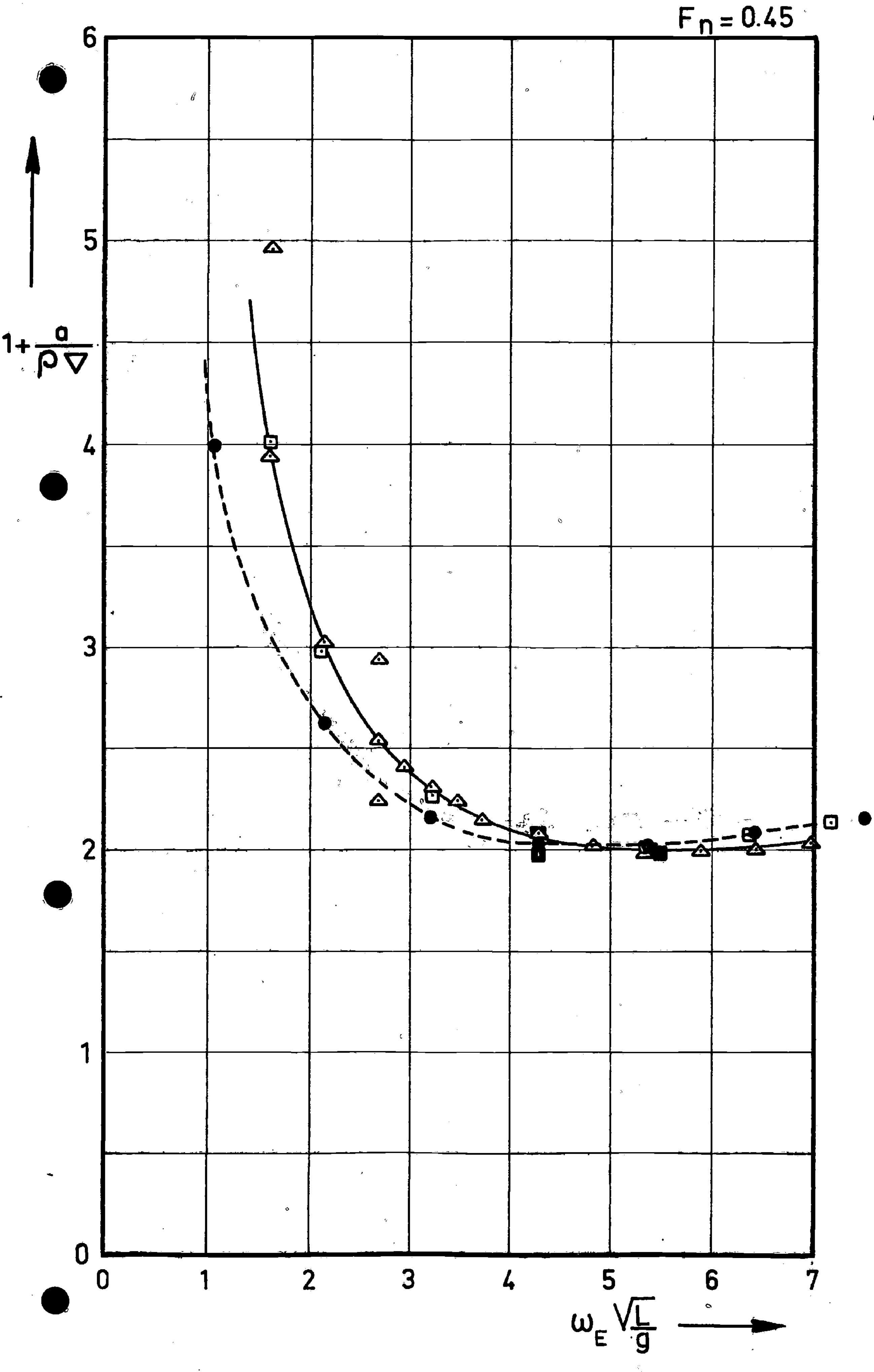

Fn = 0.45
$1+\frac{a}{\rho\nabla}$
6
5
4
3
2
1
0
0
1
2
3
4
5
6
7
$\omega_E\sqrt{\frac{L}{g}}$

FIG: 4a

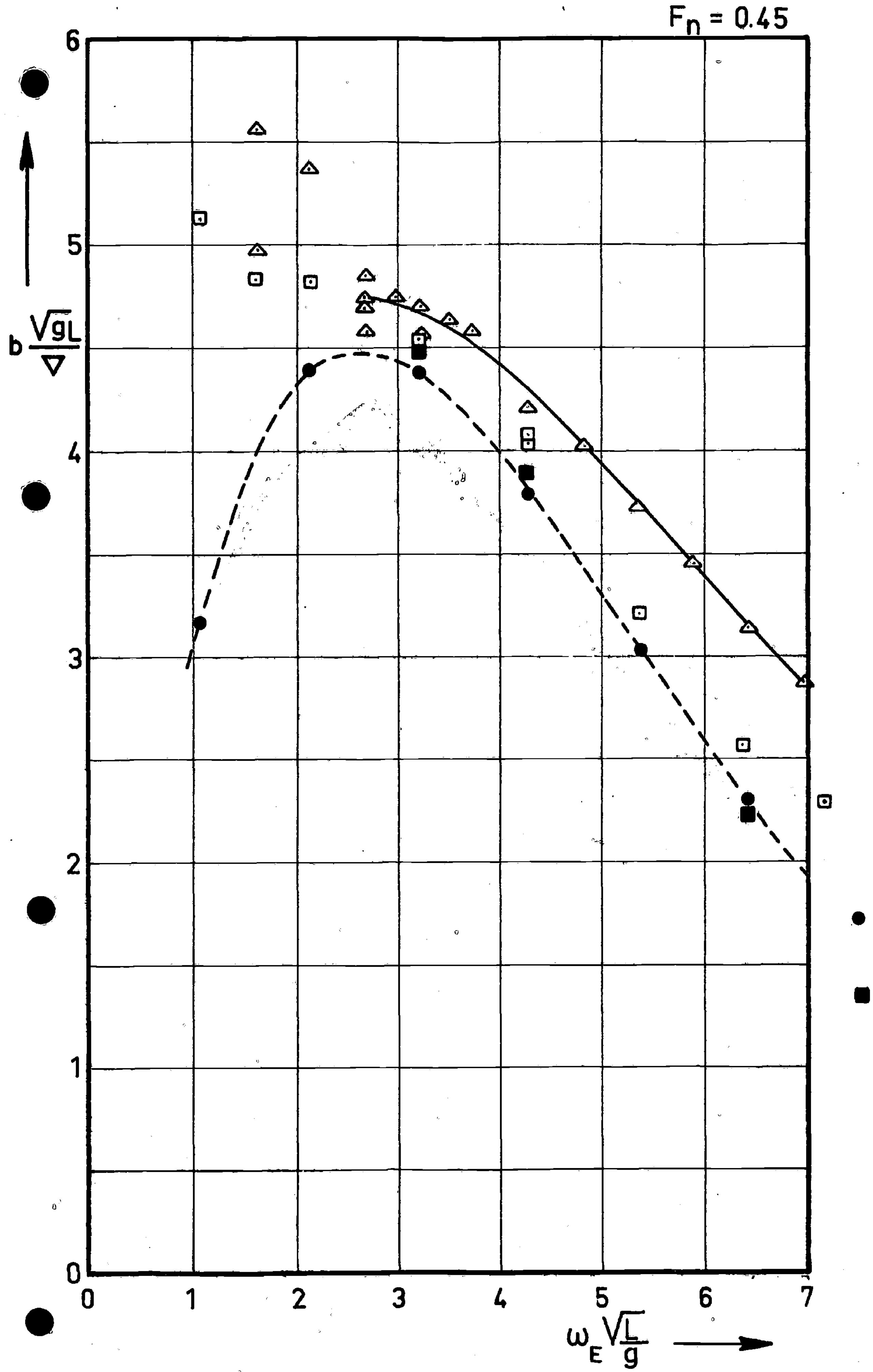

FIG: 4B

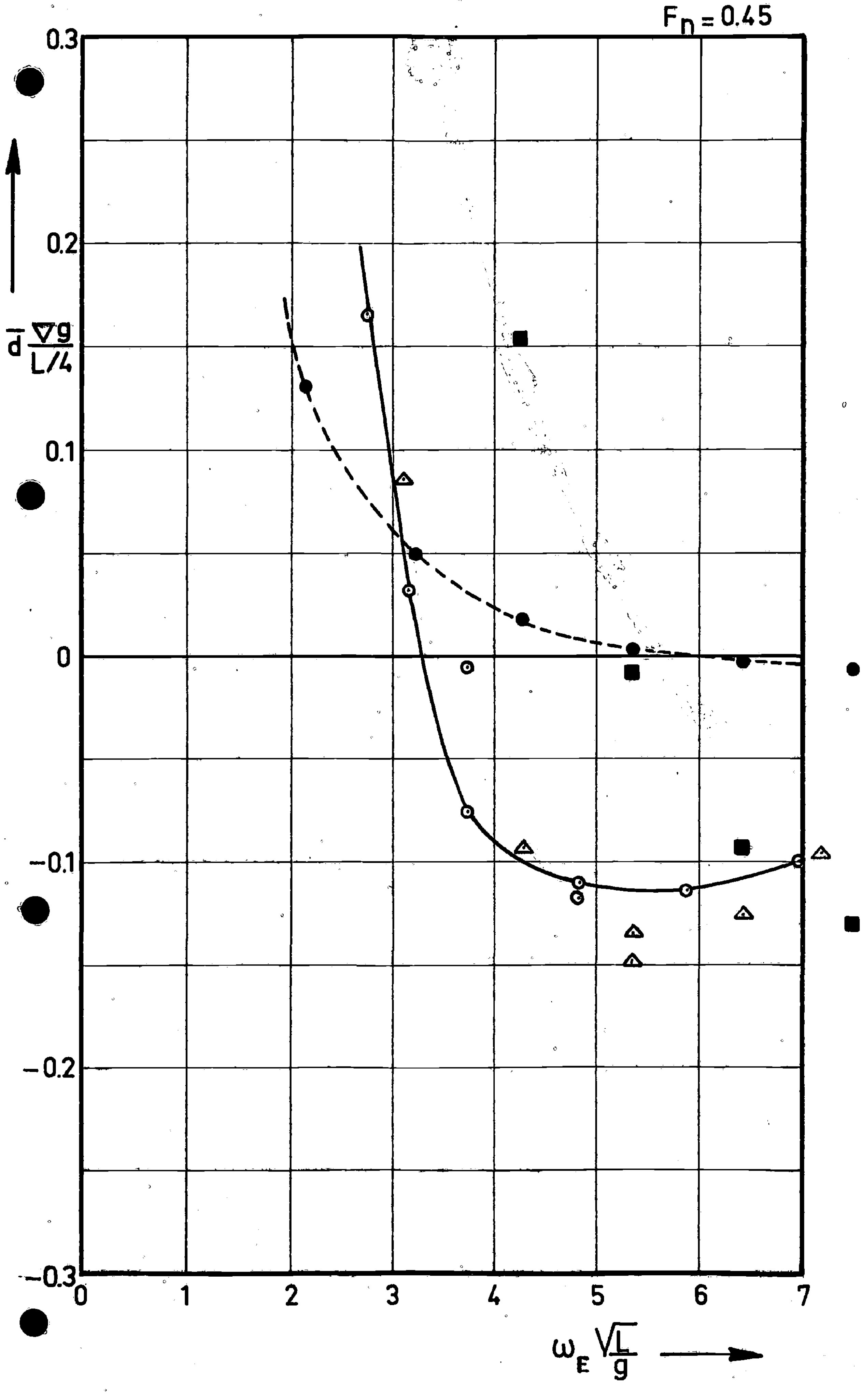

$F_n = 0.45$
0.3
0.2
0.1
0
−0.1
−0.2
−0.3
$\bar{d}\,\frac{\nabla g}{L/4}$
0
1
2
3
4
5
6
7
$\omega_E \sqrt{\frac{L}{g}}$

FIG: 4C

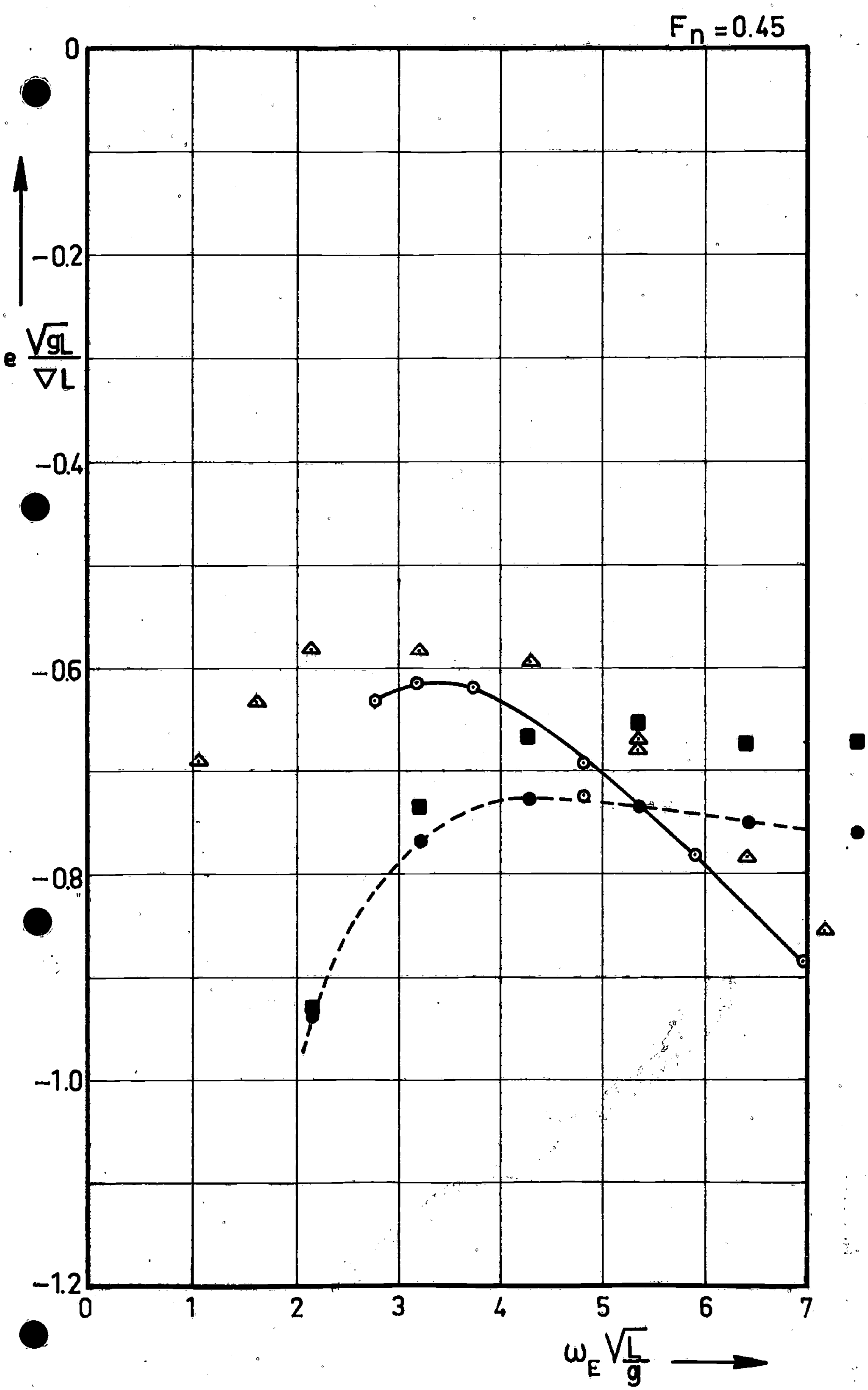

$F_n = 0.45$
$e \frac{\sqrt{gL}}{\nabla L}$
0
-0.2
-0.4
-0.6
-0.8
-1.0
-1.2
0
1
2
3
4
5
6
7
$\omega_E \sqrt{\frac{L}{g}}$

FIG: 4D

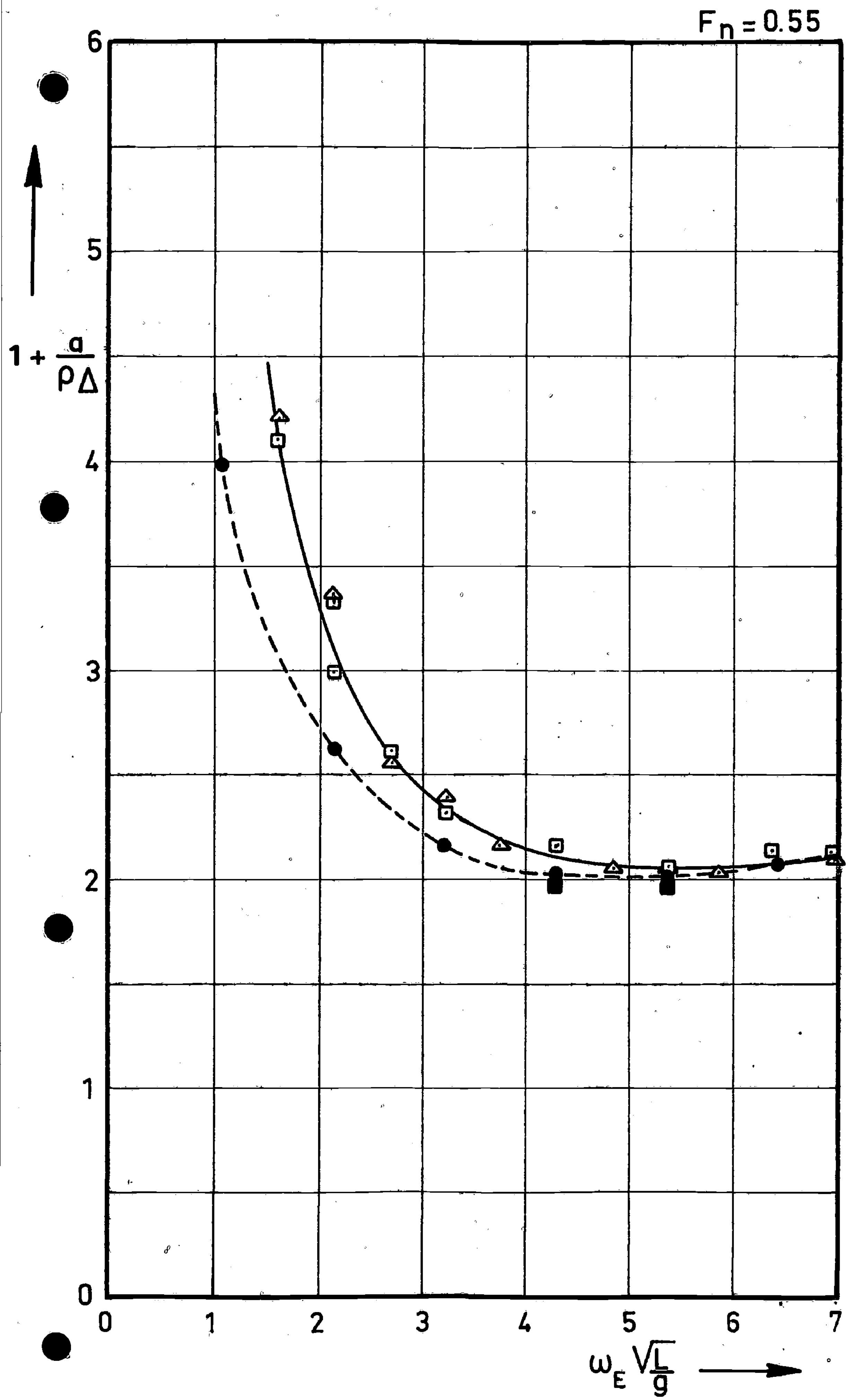

FIG: 5A

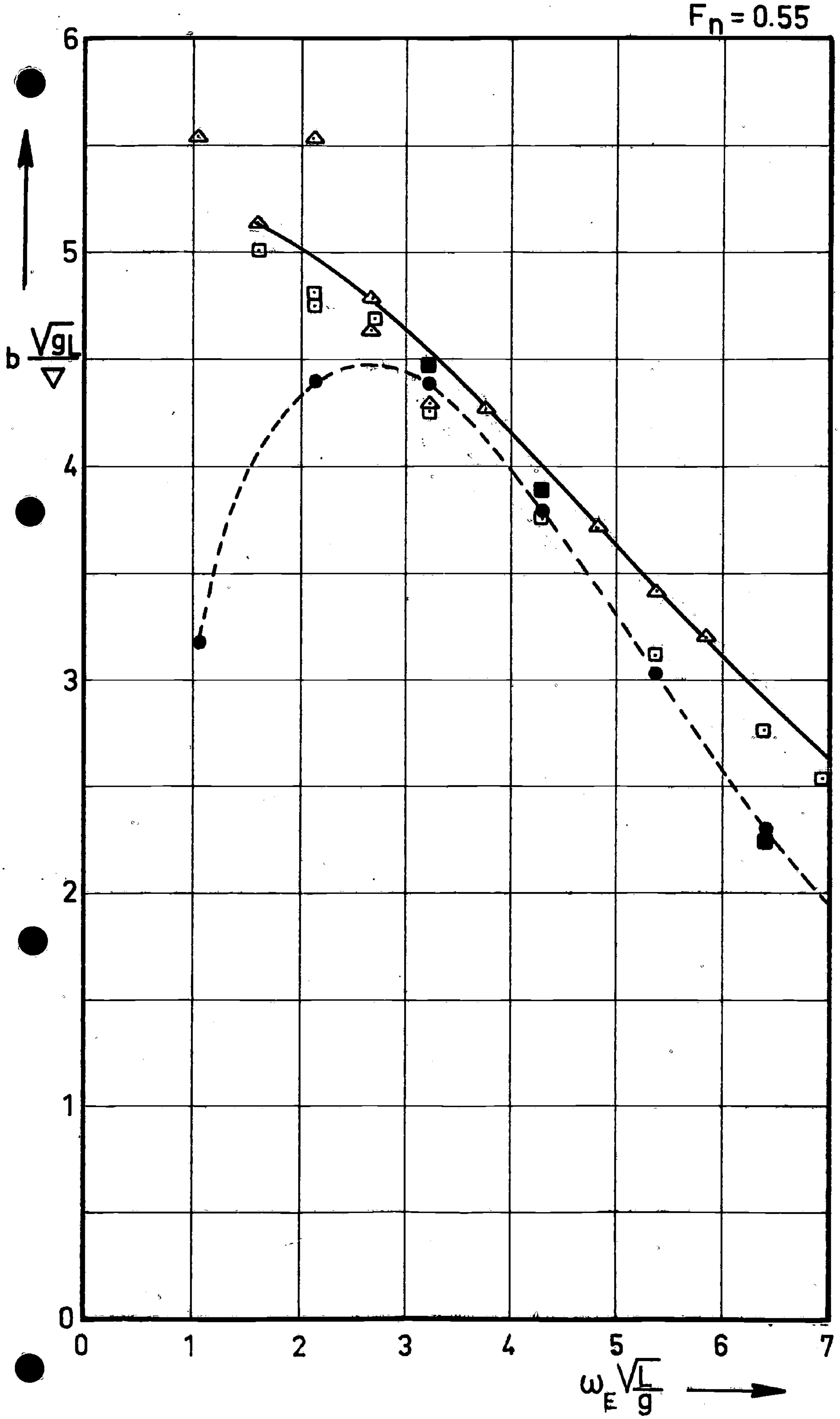

FIG: 5B

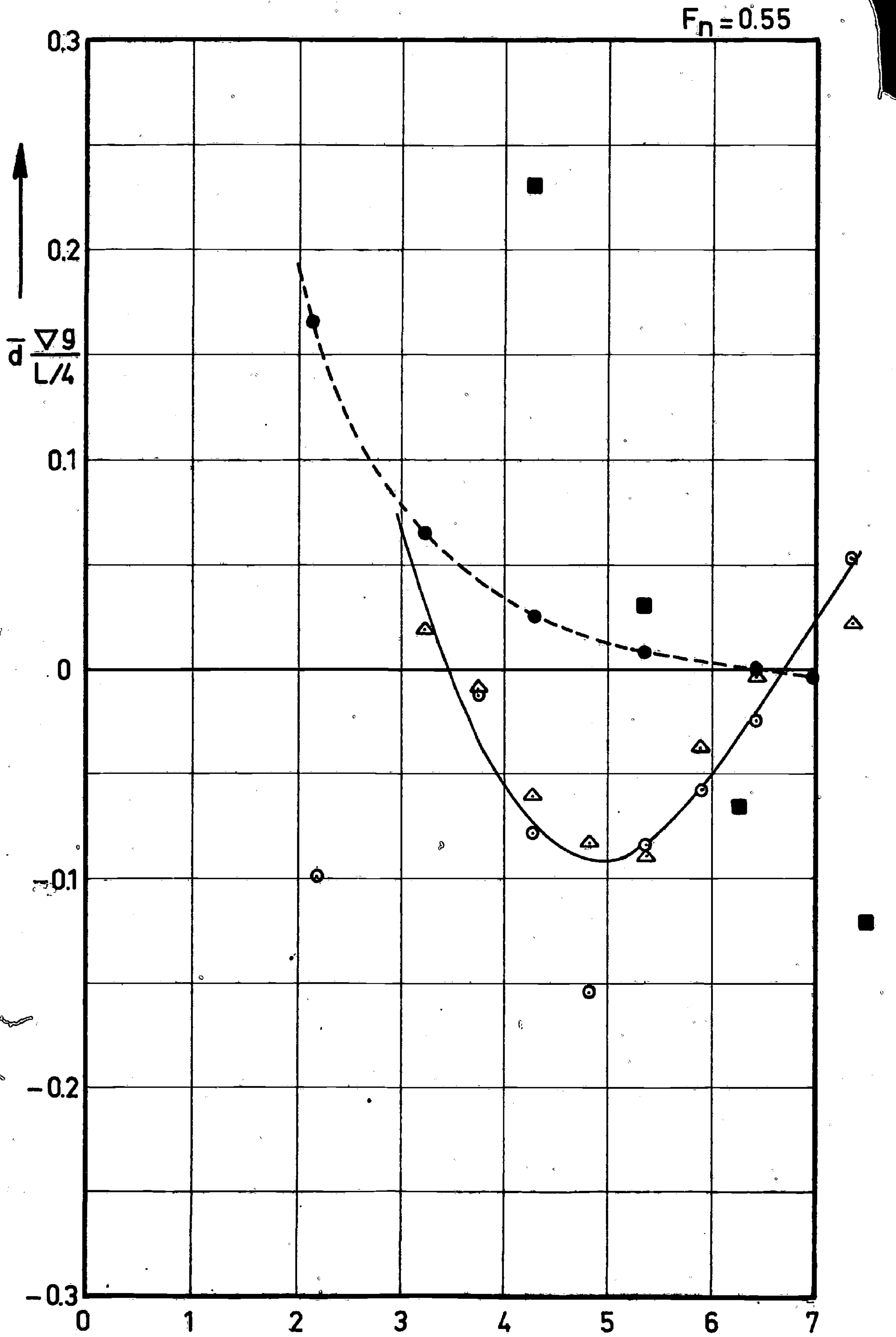

$F_n = 0.55$
$\bar{d}\,\frac{\nabla g}{L/4}$
0.3
0.2
0.1
0
−0.1
−0.2
−0.3
0
1
2
3
4
5
6
7
$\omega_E \sqrt{\frac{L}{g}}$

FIG. 5C

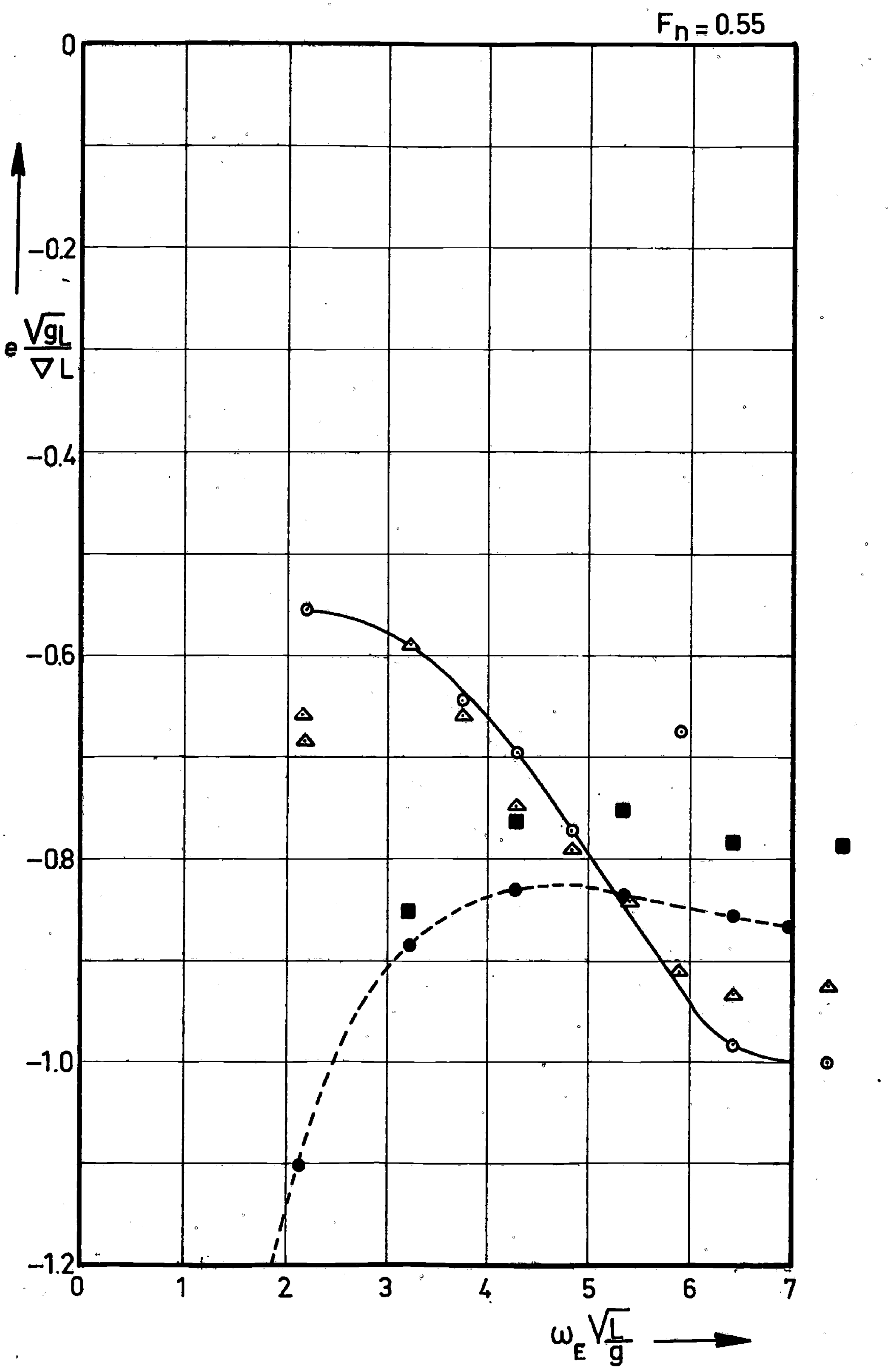

$F_n = 0.55$
0
-0.2
-0.4
-0.6
-0.8
-1.0
-1.2
$e\frac{\sqrt{gL}}{\nabla L}$
0
1
2
3
4
5
6
7
$\omega_E\sqrt{\frac{L}{g}}$

FIG: 5 D

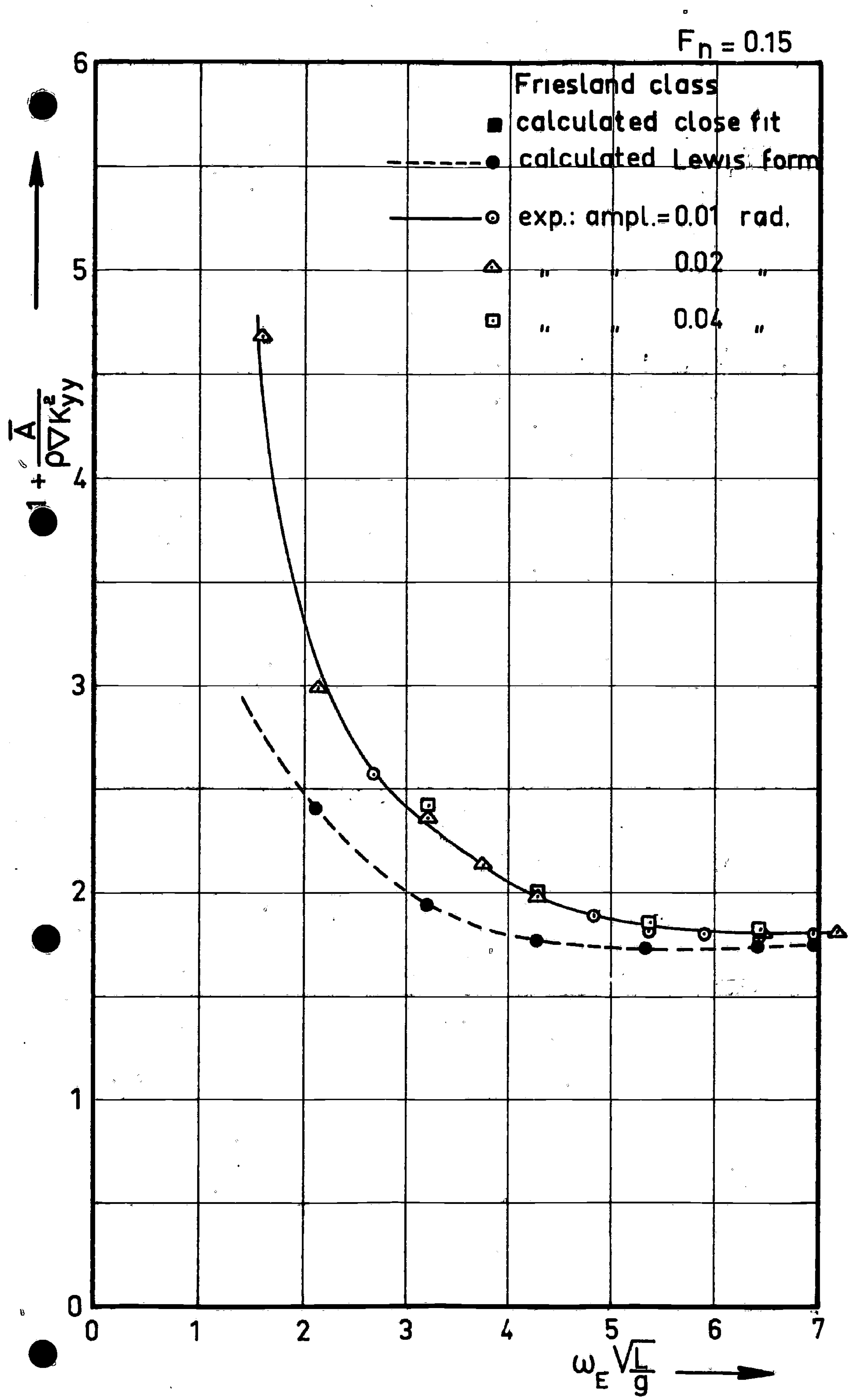

$F_n = 0.15$
Friesland class
calculated close fit
calculated Lewis form
exp.: ampl. = 0.01 rad.
" " 0.02 "
" " 0.04 "
$1 + \frac{\overline{A}}{\rho \nabla K_{yy}^2}$
$\omega_E \sqrt{\frac{L}{g}}$
0
1
2
3
4
5
6
7

FIG: 6A

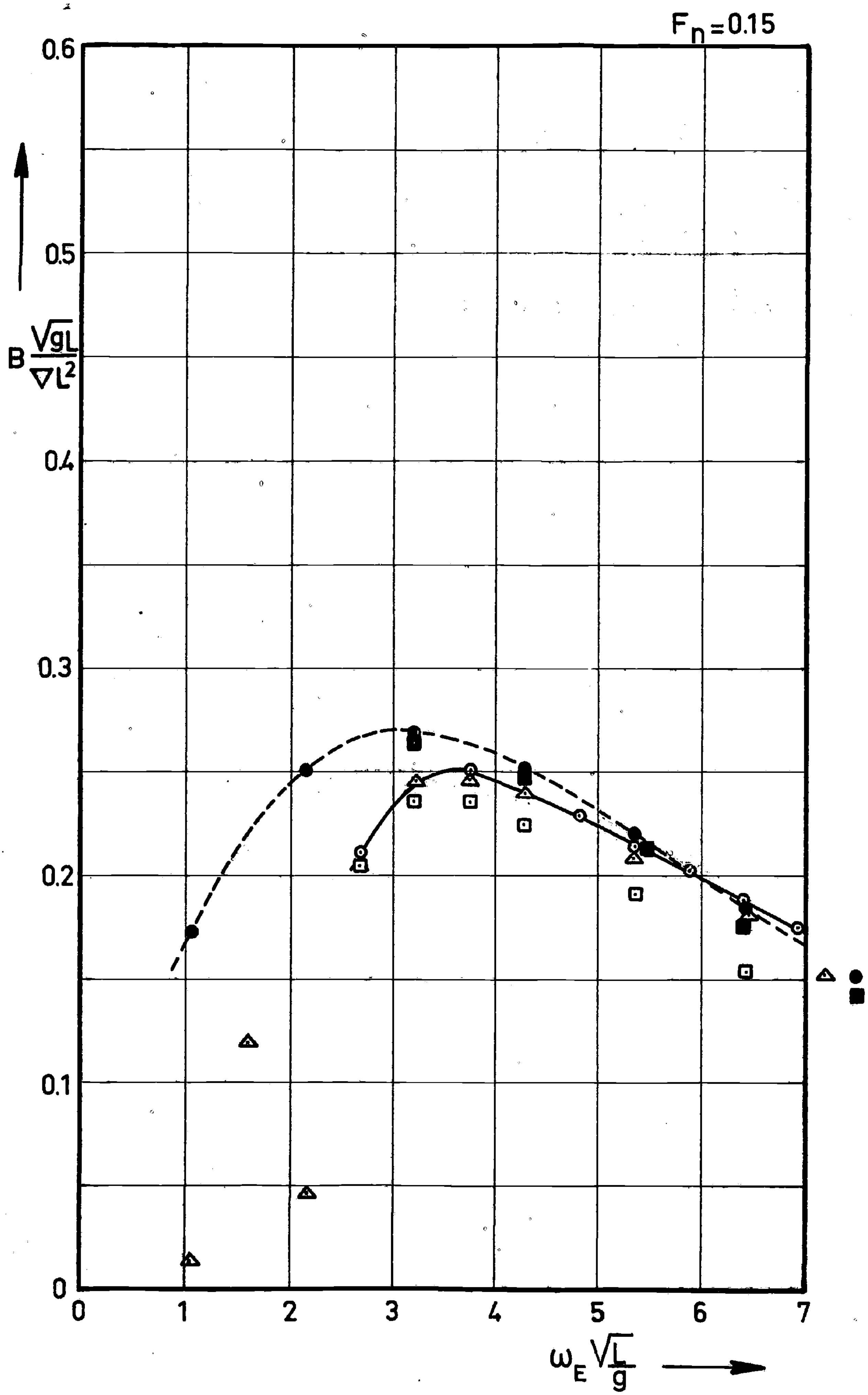

$F_n = 0.15$
0.6
0.5
0.4
0.3
0.2
0.1
0
$B \frac{\sqrt{gL}}{\nabla L^2}$
0
1
2
3
4
5
6
7
$\omega_E \sqrt{\frac{L}{g}}$

FIG: 6B

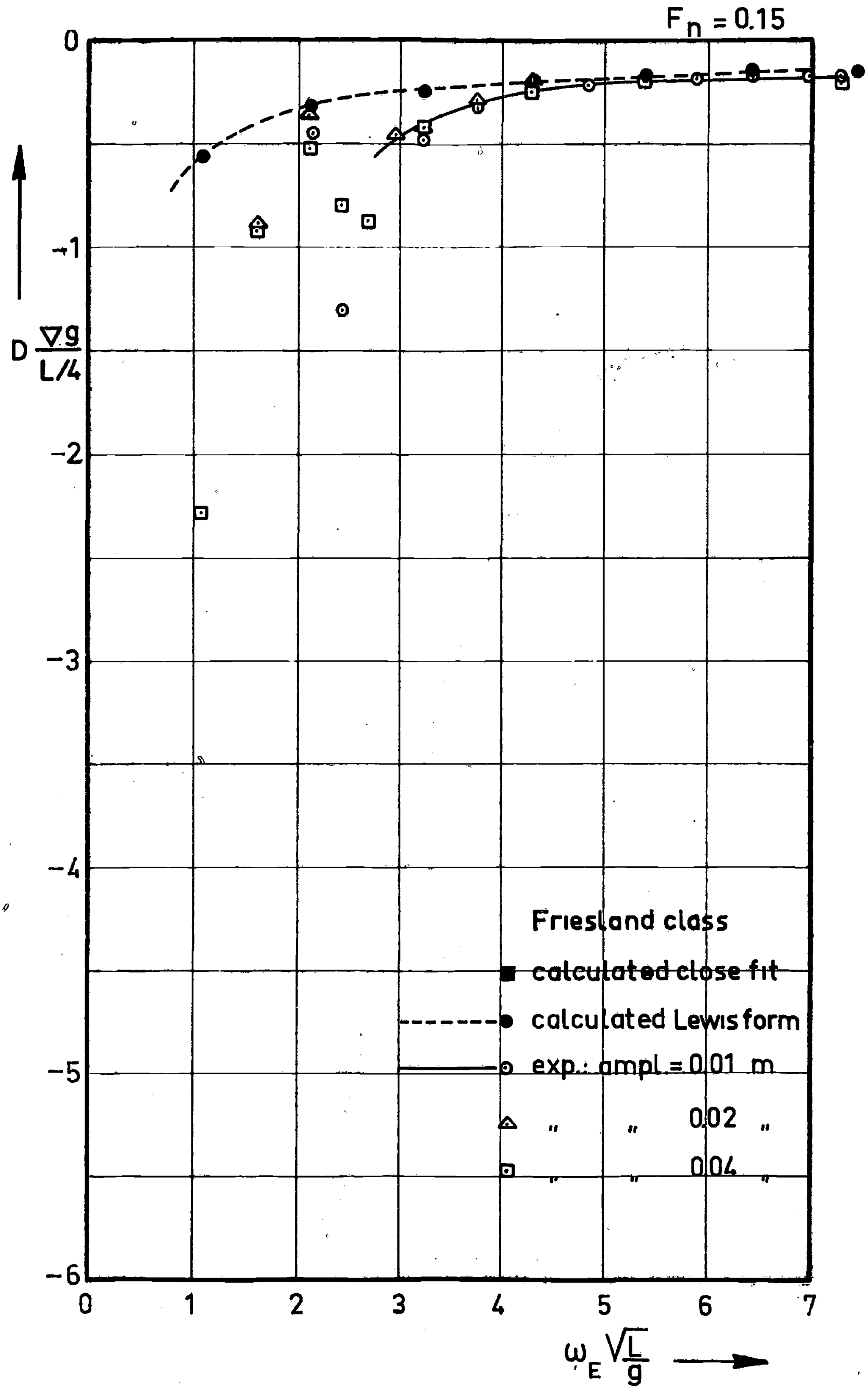

$F_n = 0.15$
0
-1
-2
-3
-4
-5
-6
$D \frac{\nabla g}{L/4}$
0
1
2
3
4
5
6
7
$\omega_E \sqrt{\frac{L}{g}}$
Friesland class
~~calculated close fit~~
calculated Lewis form
exp.: ampl. = 0.01 m
" " 0.02 "
" " 0.04 "

FIG: 6c

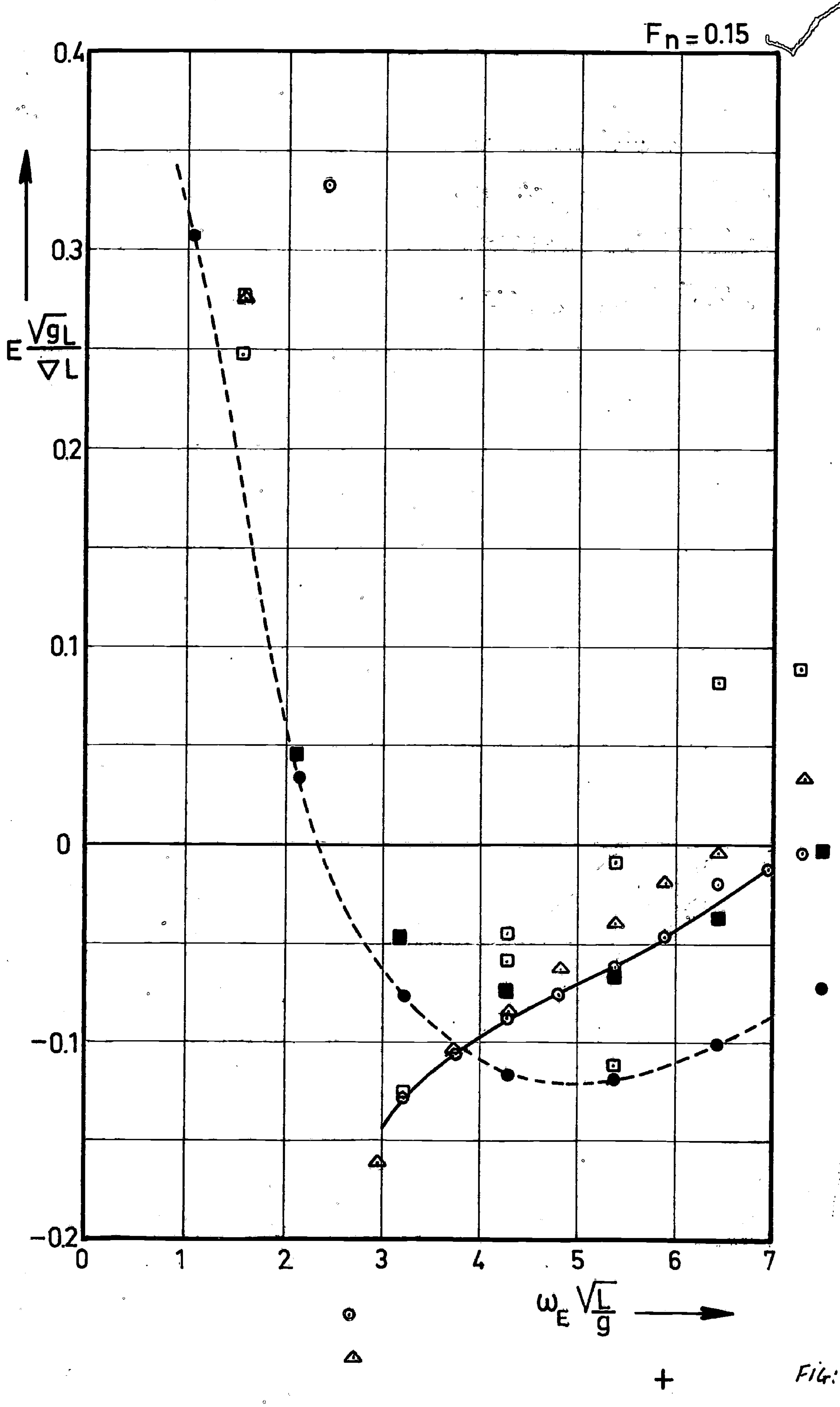

$F_n = 0.15$
0.4
0.3
0.2
0.1
0
−0.1
−0.2
$E\frac{\sqrt{gL}}{\nabla L}$
0
1
2
3
4
5
6
7
$\omega_E \sqrt{\frac{L}{g}}$

FIG: 6D

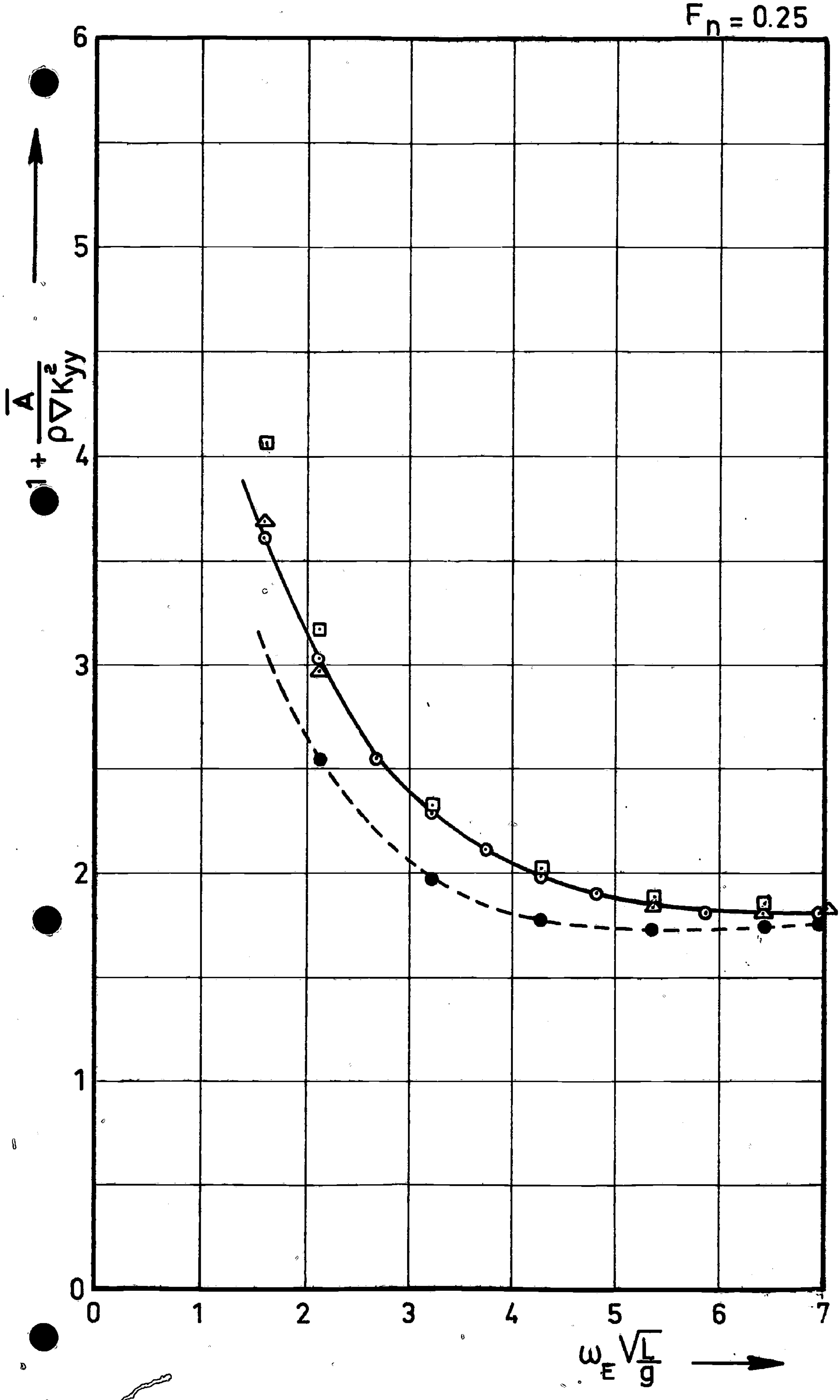

$F_n = 0.25$
$1 + \frac{\bar{A}}{\rho \nabla K_{yy}^2}$
0
1
2
3
4
5
6
7
$\omega_E \sqrt{\frac{L}{g}}$

FIG: 4a

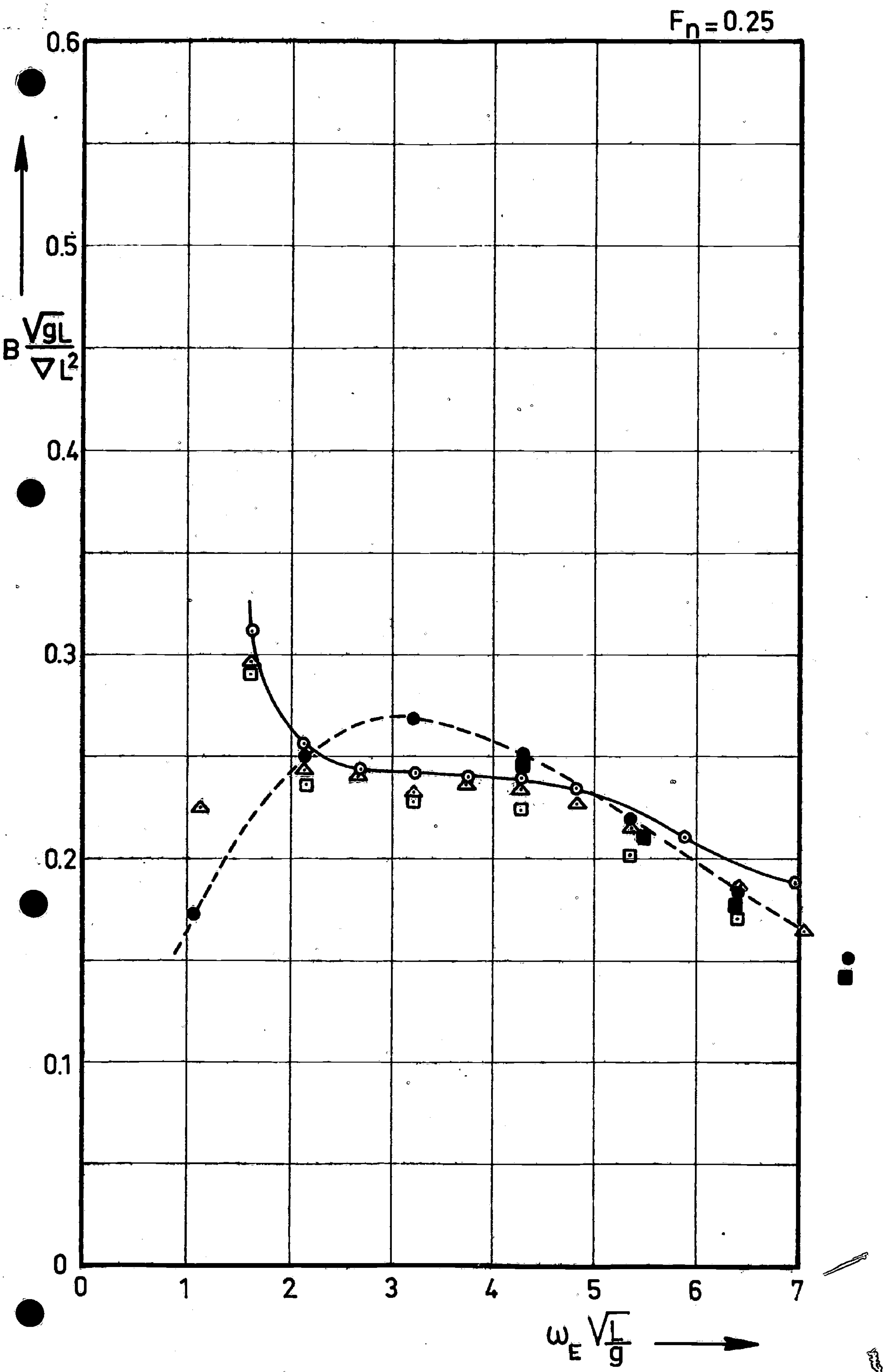

$F_n = 0.25$
$B\frac{\sqrt{gL}}{\nabla L^2}$
0.6
0.5
0.4
0.3
0.2
0.1
0
1
2
3
4
5
6
7
$\omega_E\sqrt{\frac{L}{g}}$

Fig: 4B

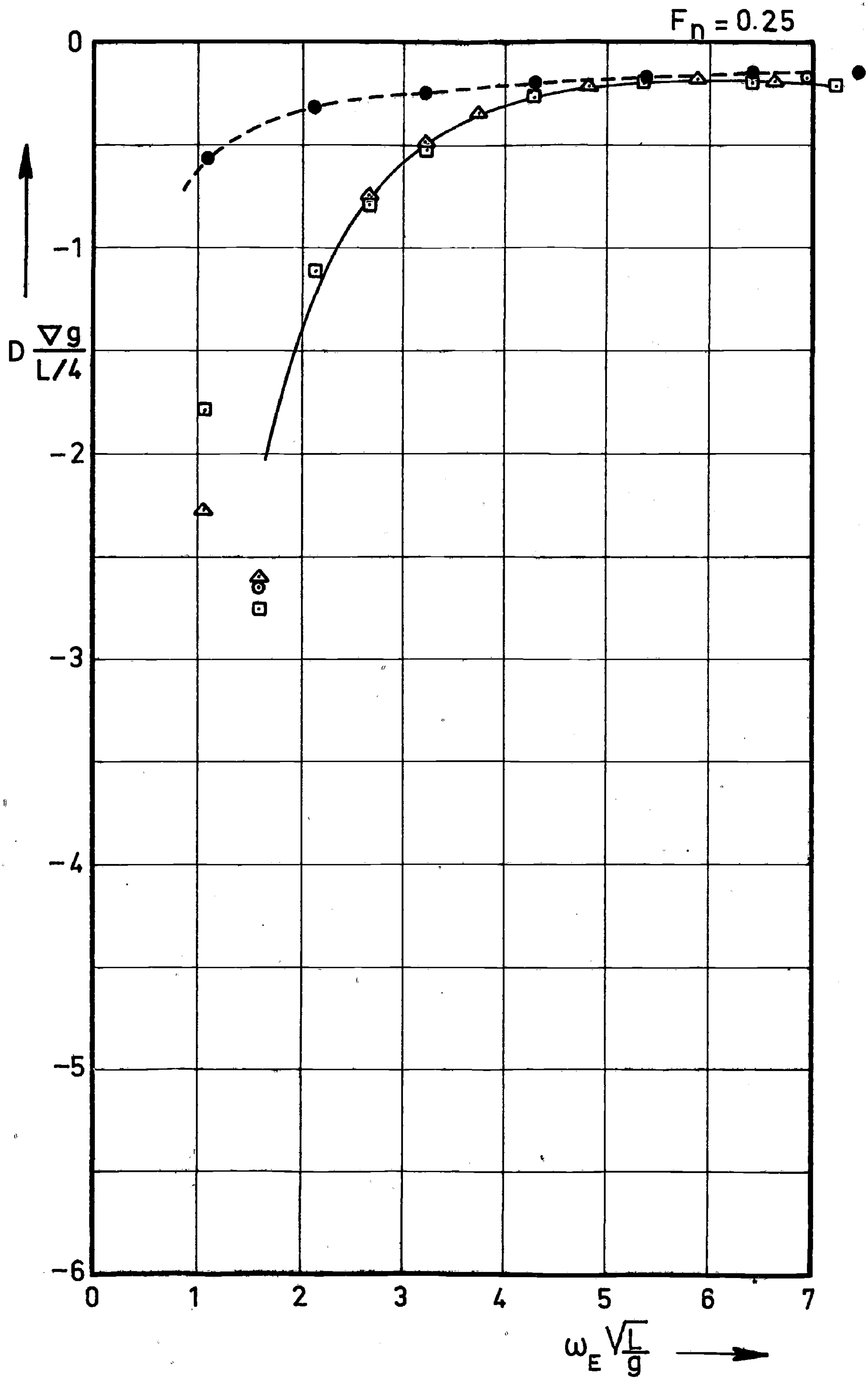

FIG: 4c.

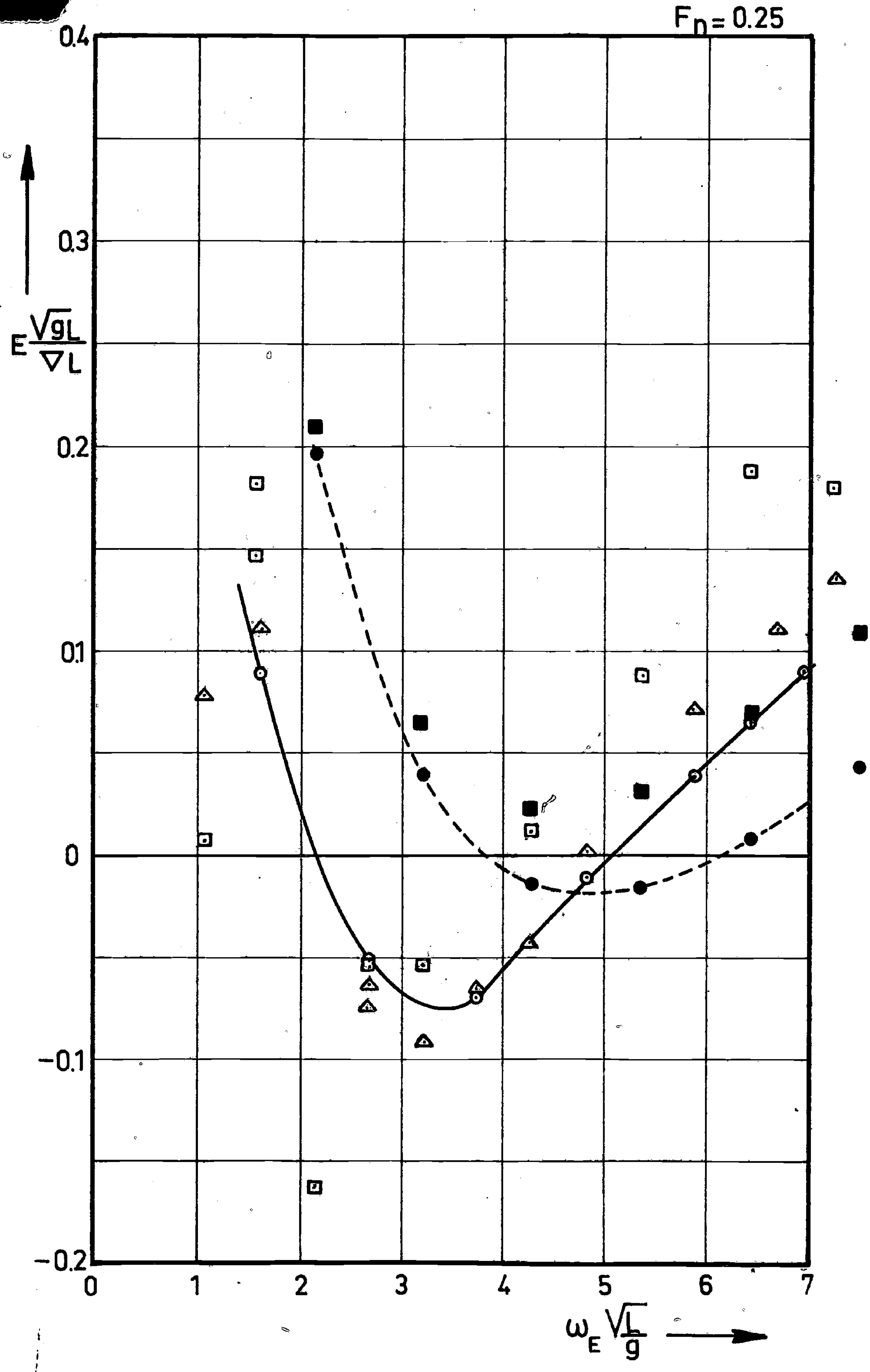
$F_n = 0.25$
0.4
0.3
0.2
0.1
0
−0.1
−0.2
$E\frac{\sqrt{gL}}{\nabla L}$
0
1
2
3
4
5
6
7
$\omega_E\sqrt{\frac{L}{g}}$

FIG: 4 D.

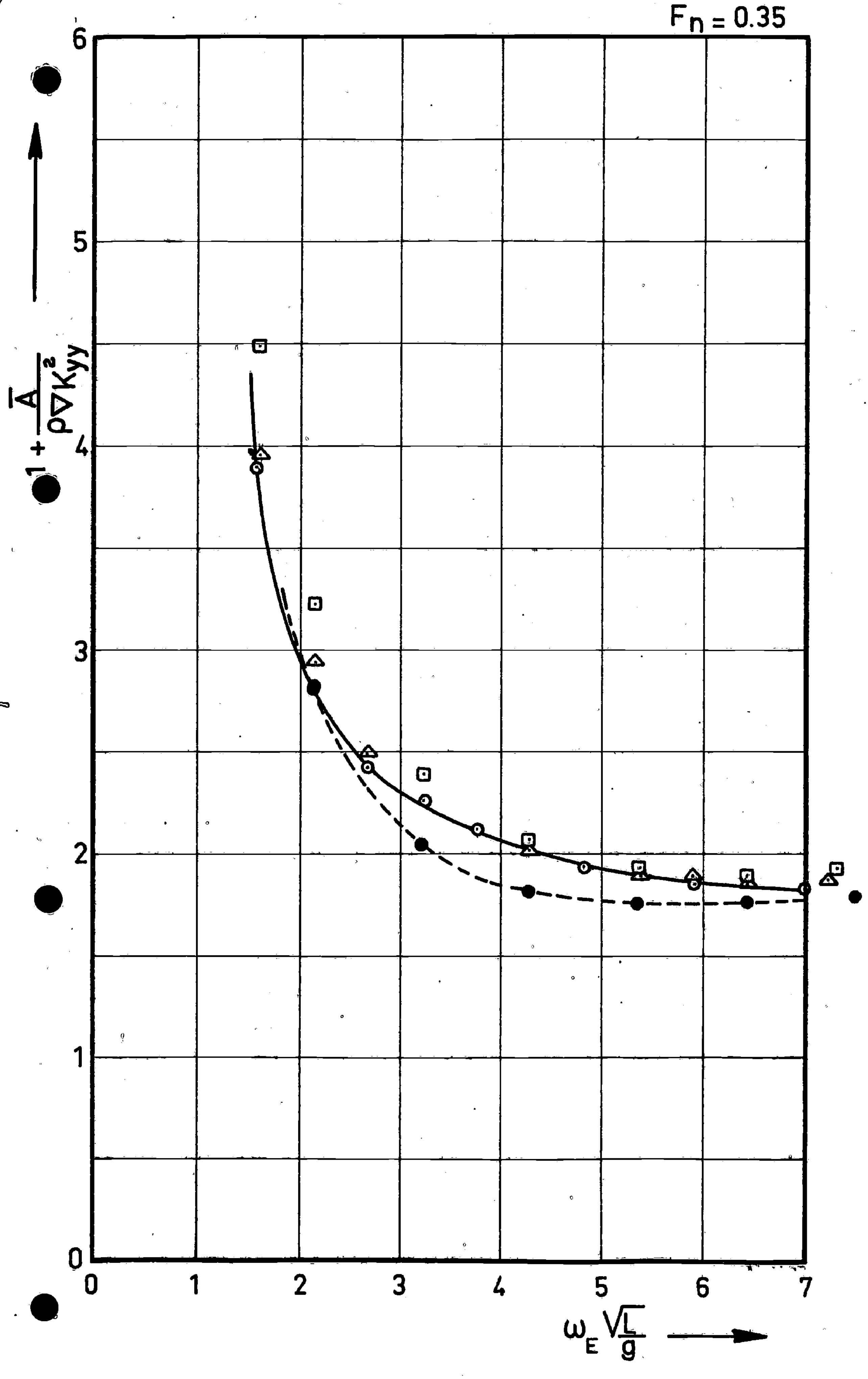

$F_n = 0.35$
$1 + \frac{\bar{A}}{\rho \nabla K_{yy}^2}$
6
5
4
3
2
1
0
0
1
2
3
4
5
6
7
$\omega_E \sqrt{\frac{L}{g}}$

FIG: 8a

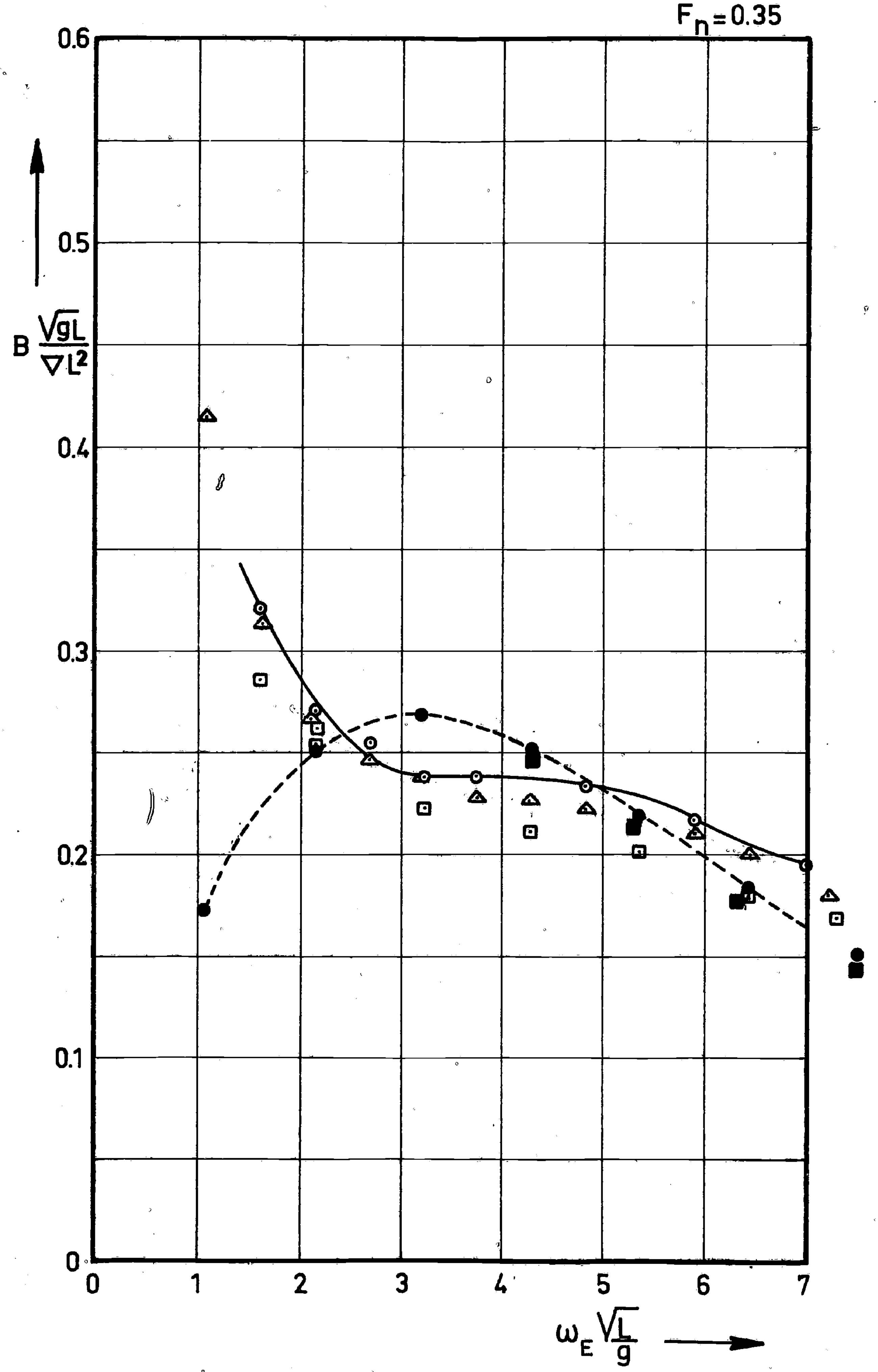
$F_n = 0.35$
$B \frac{\sqrt{gL}}{\nabla L^2}$
0.6
0.5
0.4
0.3
0.2
0.1
0
0
1
2
3
4
5
6
7
$\omega_E \sqrt{\frac{L}{g}}$

FIG: 8B

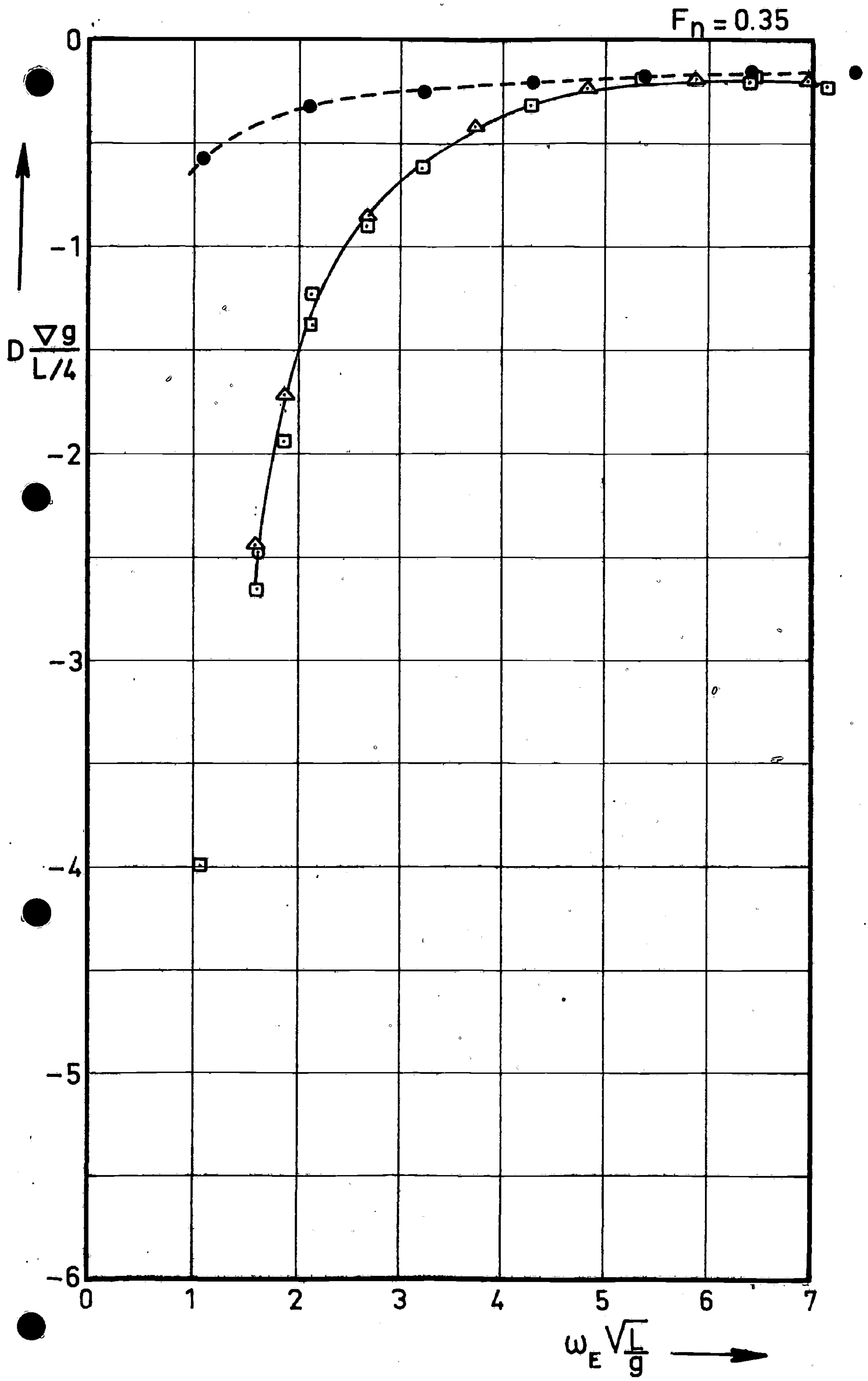

FIG: 8c

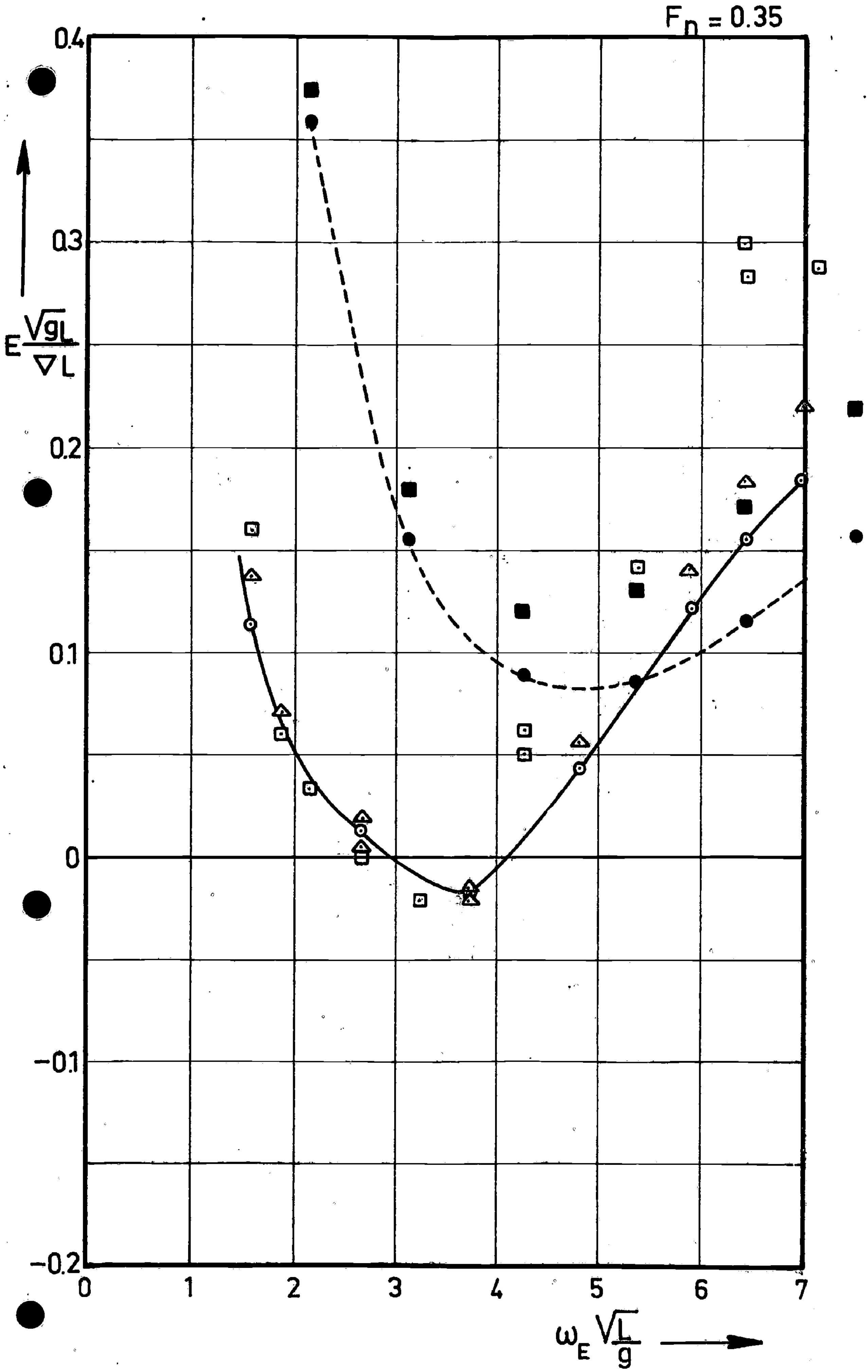
$F_n = 0.35$
0.4
0.3
0.2
0.1
0
−0.1
−0.2
$E\frac{\sqrt{gL}}{\nabla L}$
0
1
2
3
4
5
6
7
$\omega_E \sqrt{\frac{L}{g}}$

Fig: 8D

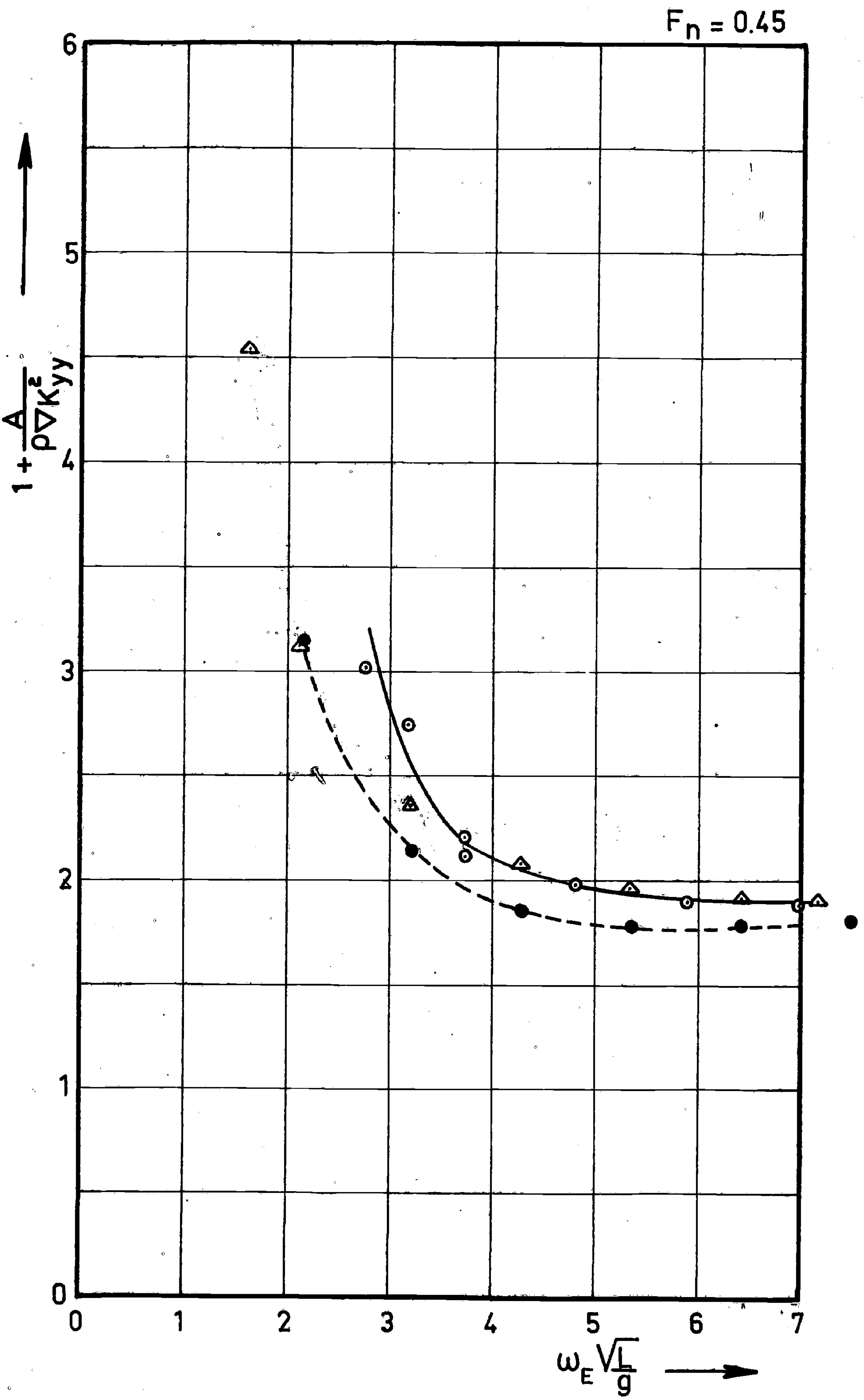

$F_n = 0.45$
$1 + \frac{\bar{A}}{\rho \nabla K_{yy}^2}$
$\omega_E \sqrt{\frac{L}{g}}$
0
1
2
3
4
5
6
7

FIG: 9A

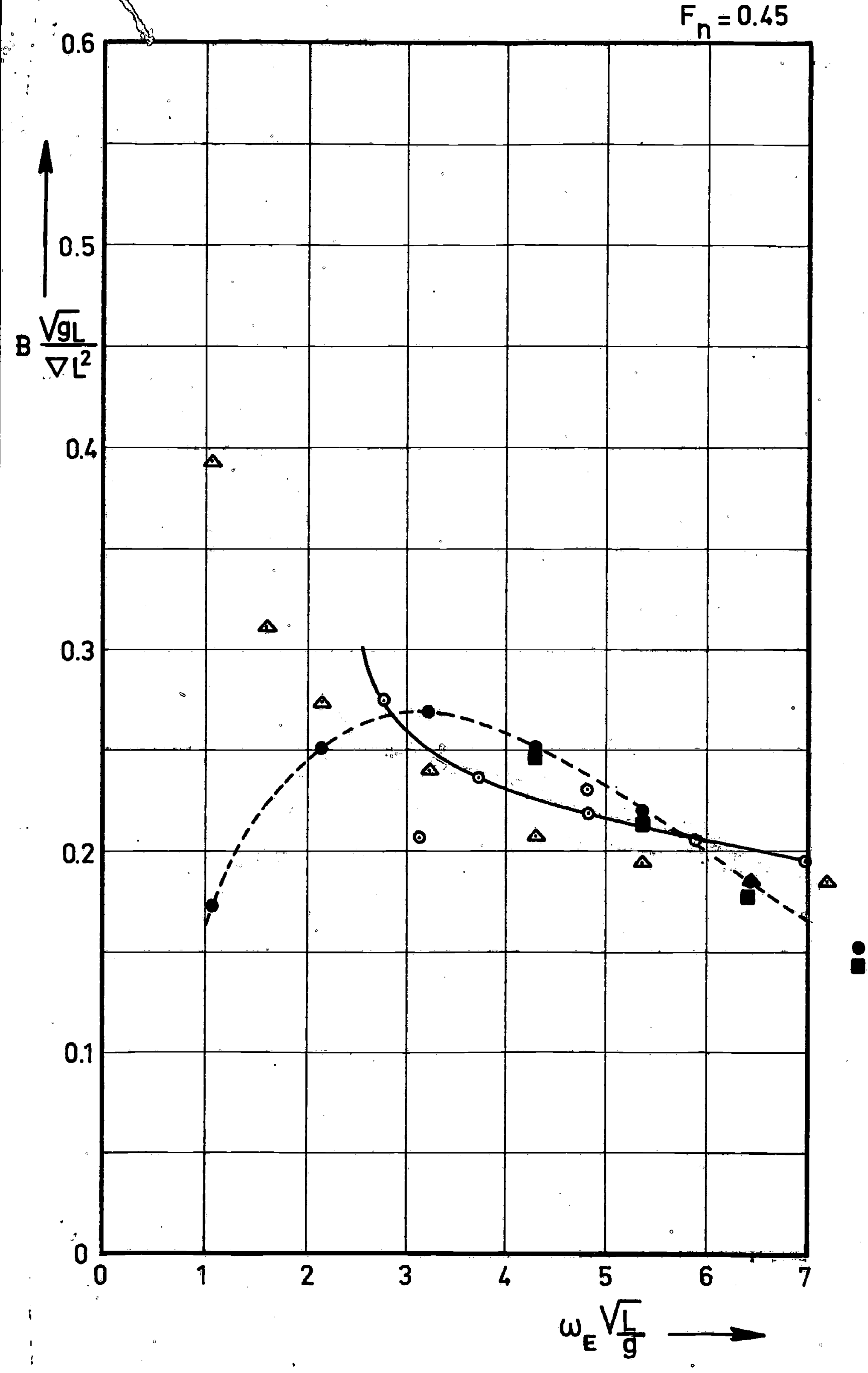
$F_n = 0.45$
0.6
0.5
$B \frac{\sqrt{gL}}{\nabla L^2}$
0.4
0.3
0.2
0.1
0
0
1
2
3
4
5
6
7
$\omega_E \sqrt{\frac{L}{g}}$

Fig: 9 B

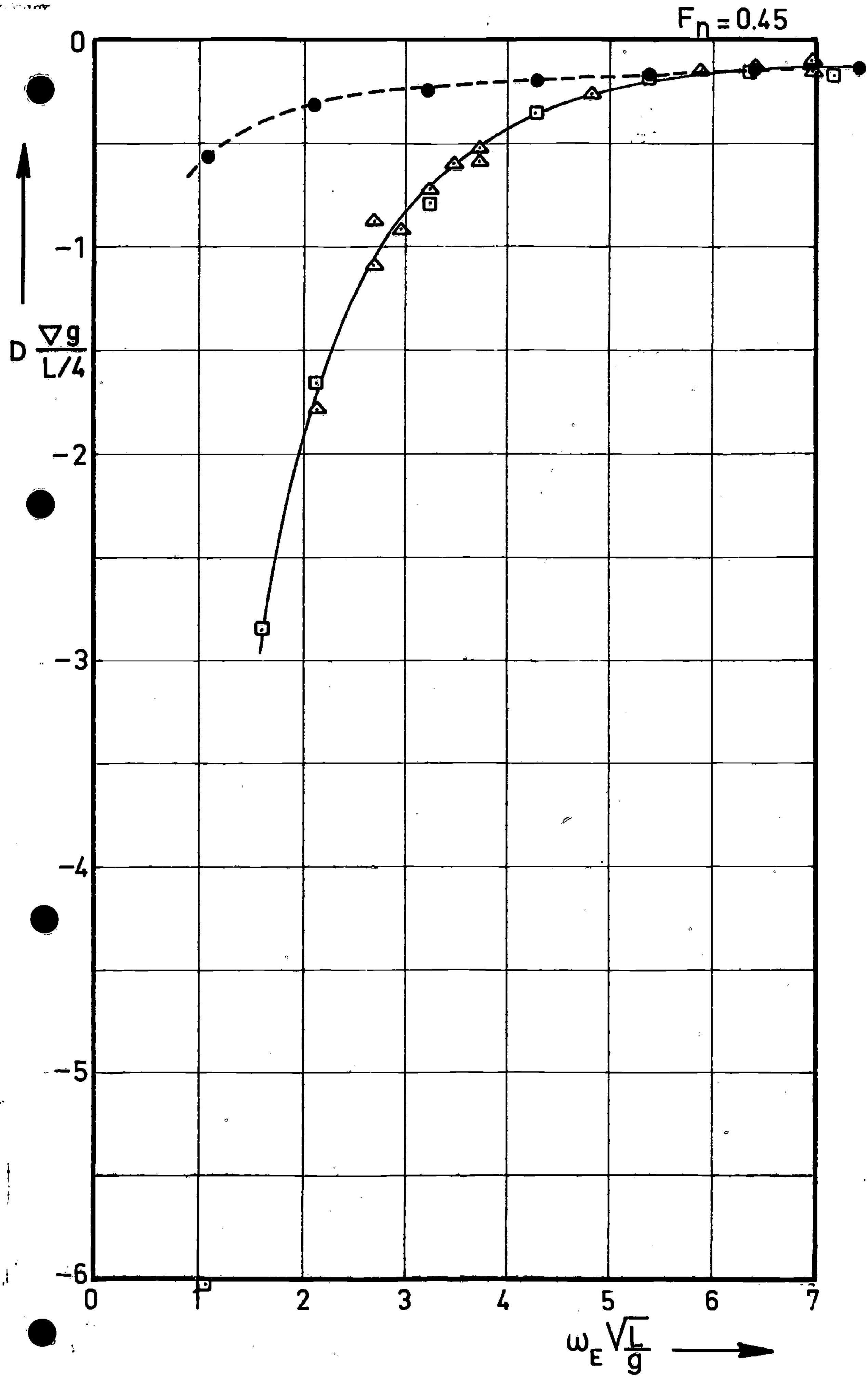

FIG. 9c

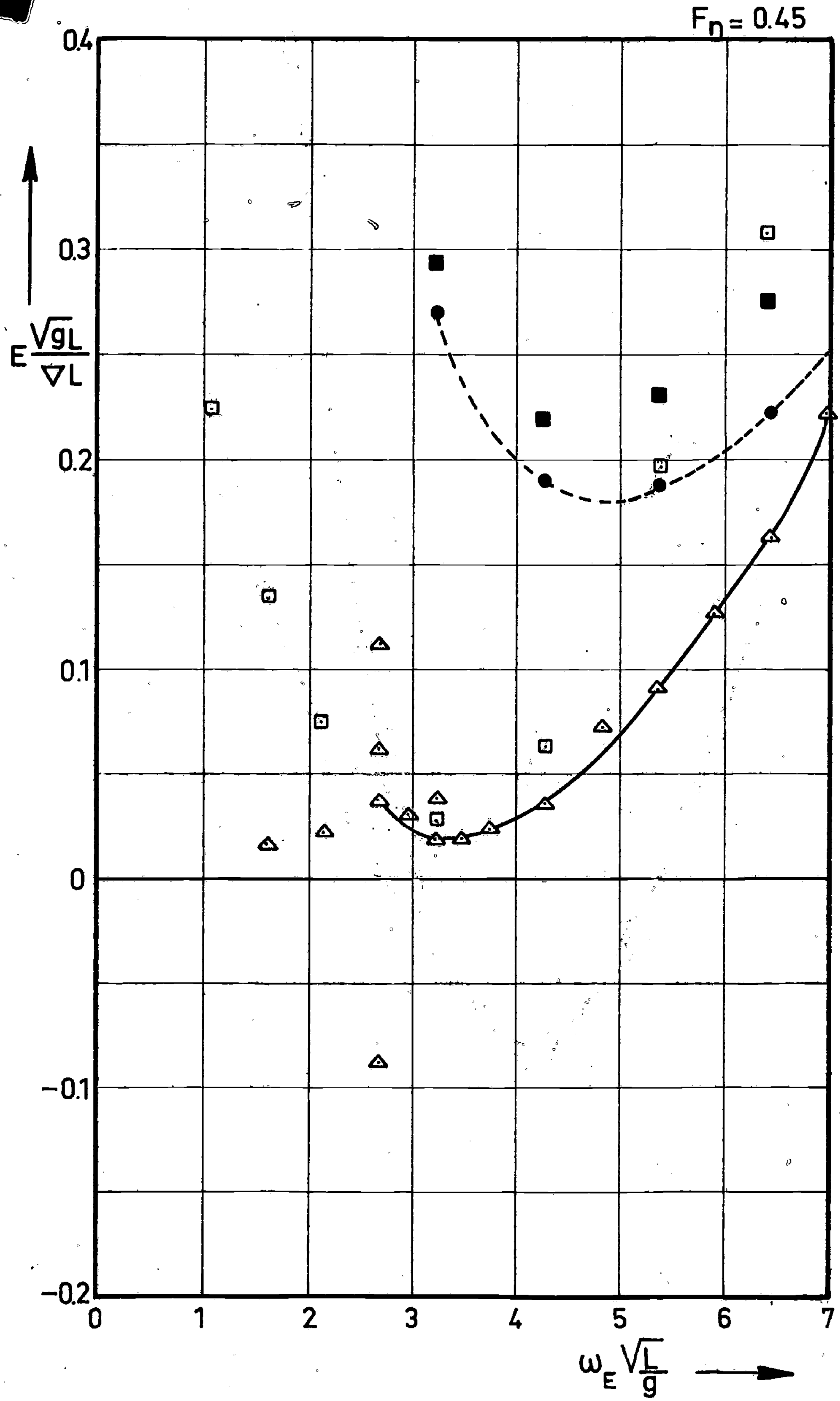

FIG. 9D

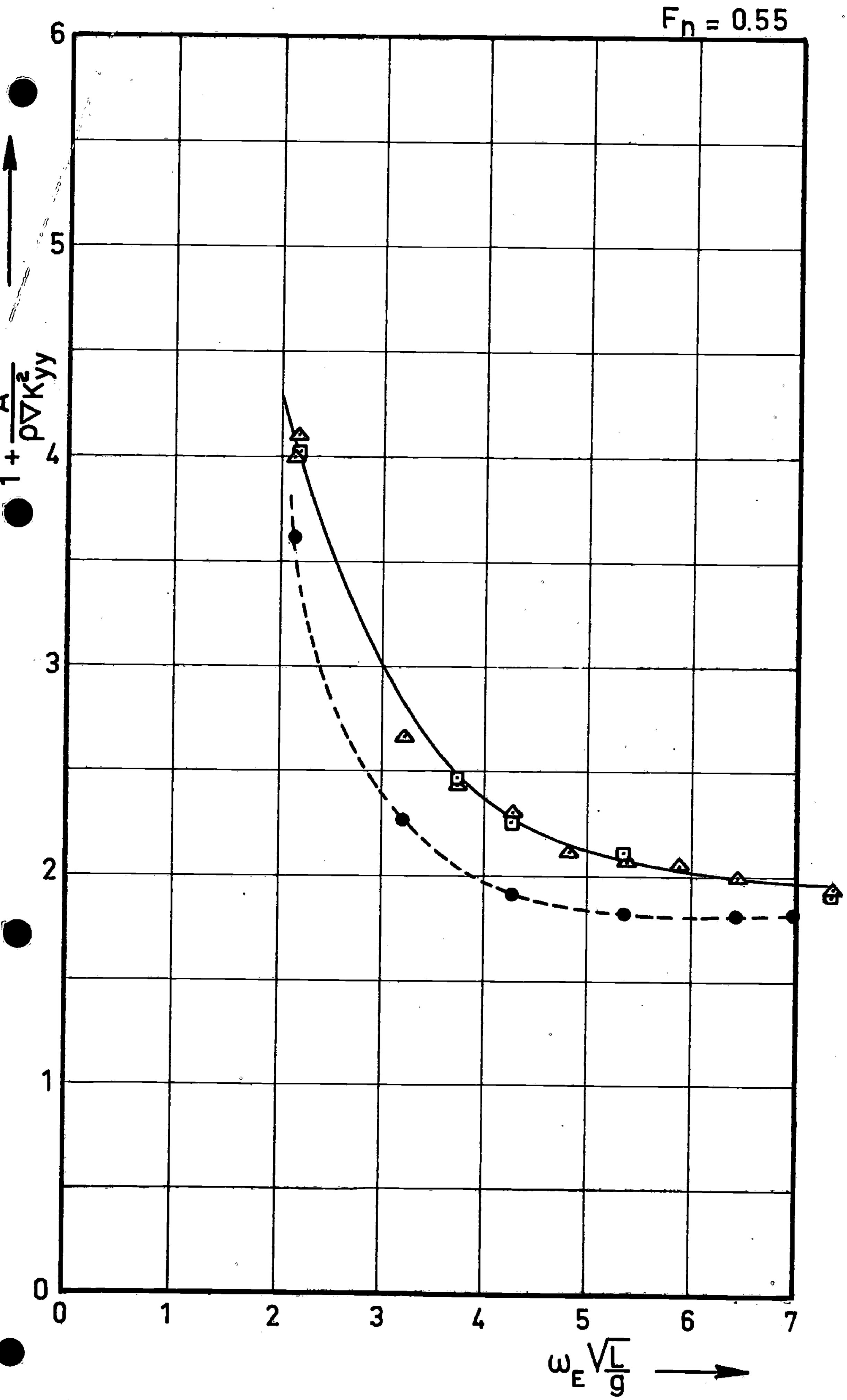

$F_n = 0.55$
$1 + \frac{\bar{A}}{\rho \nabla K_{yy}^2}$
$\omega_E \sqrt{\frac{L}{g}}$
0
1
2
3
4
5
6
7

FIG: 10 A

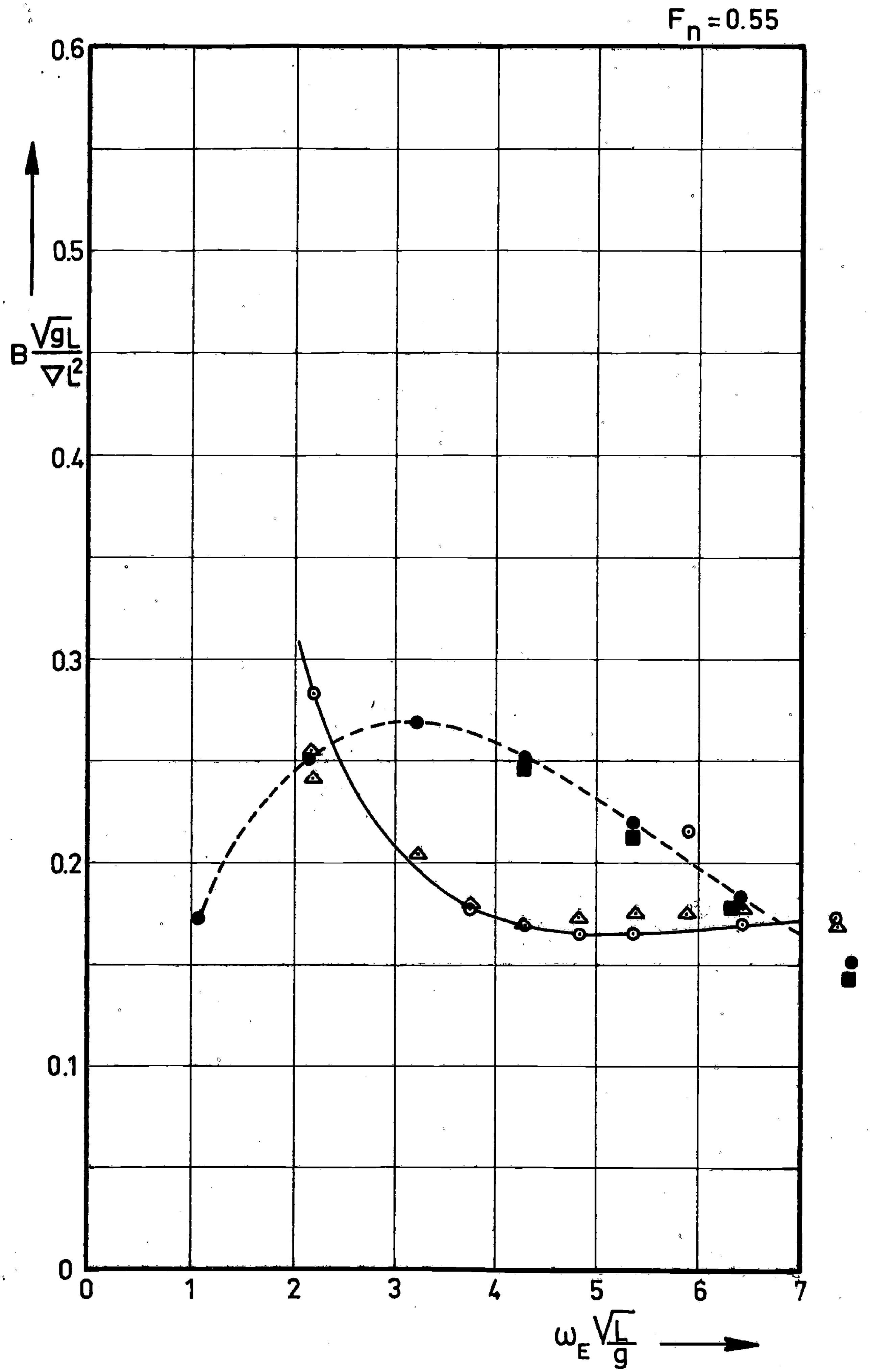

$F_n = 0.55$
0.6
0.5
0.4
0.3
0.2
0.1
0
$B\frac{\sqrt{gL}}{\nabla L^2}$
0
1
2
3
4
5
6
7
$\omega_E\sqrt{\frac{L}{g}}$

FIG: 10 B

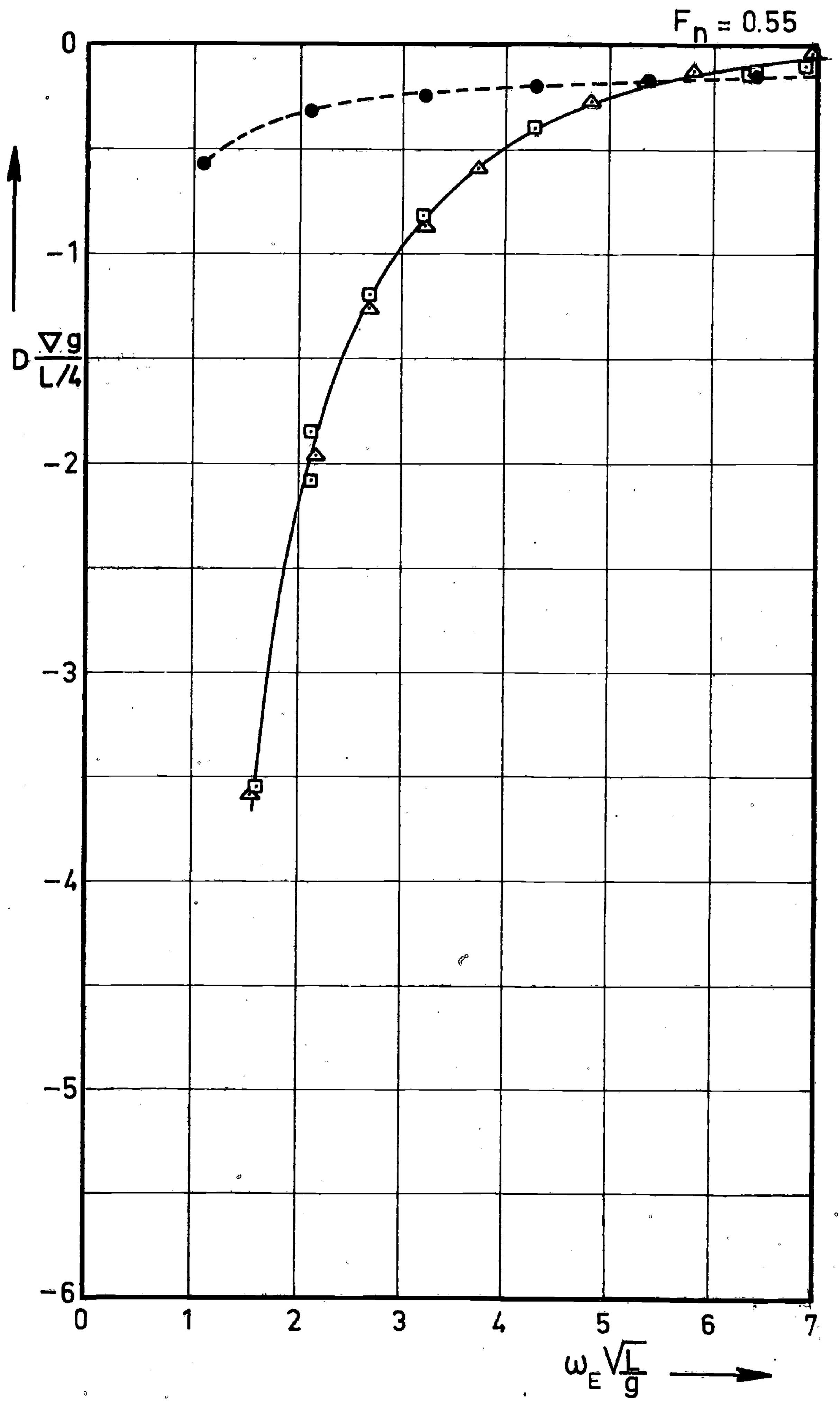

FIG: 10 c

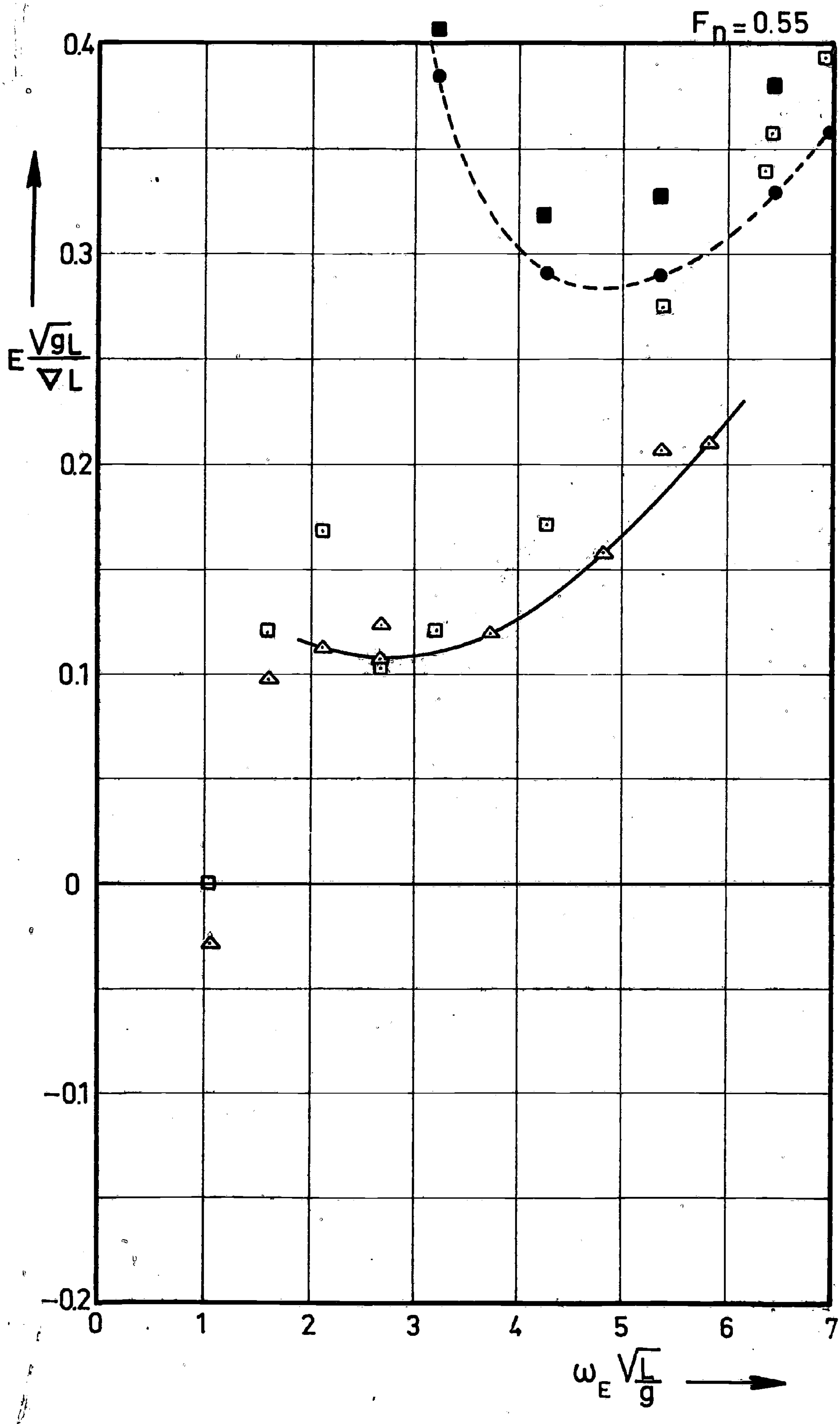

$F_n = 0.55$
$E\frac{\sqrt{gL}}{\nabla L}$
0.4
0.3
0.2
0.1
0
-0.1
-0.2
0
1
2
3
4
5
6
7
$\omega_E\sqrt{\frac{L}{g}}$

FIG 10D

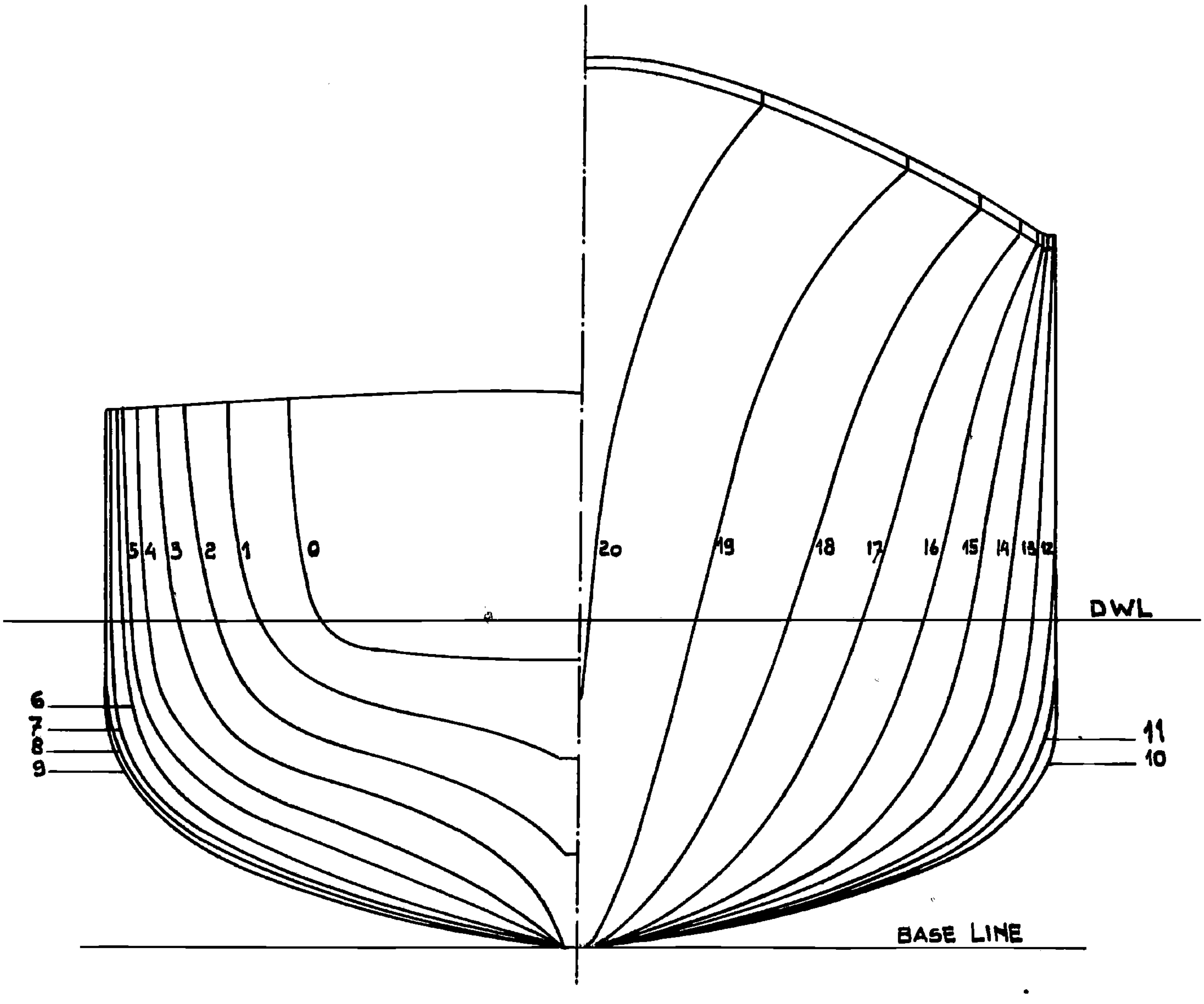

FRIESLAND CLASS FRIGATE

FIGURE